Table of contents

Supplementary Notes 3

Supplementary Methods 6

Supplementary Table Legends 14

Supplementary Figures 16

Figure S1. The distribution of platelet counts and the 0.5th and 2.5th percentiles during the first, second, and third trimesters, at delivery, and during the postpartum period from two cohorts. 16

Figure S2. QQ plots of GWAS meta-analyses of platelet count during pregnancy, at delivery, and during the postpartum period. 17

Figure S3. The number of genome-wide significant loci and signals for the GWAS meta-analyses of platelet count during pregnancy, at delivery, and during the postpartum period. 18

Figure S4. The number of genome-wide significant loci and signals for platelet count during the first, second, and third trimesters. 19

Figure S5. Manhattan plots and QQ plots for GWAS of platelet count at delivery and during the postpartum period. 20

Figure S6. Comparing GWAS of platelet count during pregnancy, at delivery, and during the postpartum period of Longgang to Baoan. 21

Figure S7. Regional association plots for novel loci of GWAS meta-analyses of platelet count during pregnancy, at delivery, and during the postpartum period. 22

Figure S8. Comparing GWAS meta-analyses of platelet count during pregnancy, at delivery, and during the postpartum period to the GWAS summary statistics of platelet count in BBJ. 24

Figure S9. The result of co-localization between the GWAS of platelet count of the five periods of pregnancy and the platelet count in BBJ. 25

Figure S10. Regional association plots for five loci with the smallest PPH4 values in the co-localization analysis. 27

Figure S11. Distribution of the number of repeated measurements of platelet counts in Baoan and Longgang. 28

Figure S12. TrajGWAS results of the mean of longitudinal platelet count during pregnancy and the postpartum period. 29

Figure S13. TrajGWAS results of the within-subject variability of longitudinal platelet counts during pregnancy and the postpartum period. 30

Figure S14. Receiver operating characteristic (ROC) curves of 8 models for GT 31

Figure S15. Regional association plots and LD heatmap of GT in *PEAR1* locus.....32

Figure S16. Regional association plots for novel loci of GWAS meta-analyses of GT. 35

Figure S17. Regional association plots of rs12041331 and rs12276986 for platelet count at delivery and during the postpartum period. 36

Figure S18. Mean platelet counts over gestation age.....37

Figure S20. Mean platelet volumes over gestation age.....39

Figure S23. TrajGWAS results of the mean of longitudinal MPV during pregnancy and the postpartum period.....43

Figure S24. TrajGWAS results of the within-subject variability of longitudinal MPV during pregnancy and the postpartum period.....44

Supplementary Notes

Factors influencing GT during pregnancy

We primarily focused on prenatal screening indicators readily obtainable during the first trimester, such as BMI, SBP, and DBP. We also compared the mode of conception within severe GT cases, mild GT cases, and control pregnancies. Several early pregnancy factors were associated with the mean platelet and GT during pregnancies. The age of severe GT was higher than mild GT and controls (both $P < 2.2\times10^{-16}$). The difference in BMI, SBP, and DBP of the first trimester among control, mild GT, and severe GT was relatively small but statistically significant. There were more pregnancies conceived with in vitro fertilization in the two GT groups (mild GT: 4.5%, P = 0.011, and severe GT: 5.6%, P = 0.031) (**Table S1**).

Maternal and neonatal pregnancy outcomes of GT

We compared maternal and neonatal outcomes among control and GT pregnancies (**Table S23**). The proportion of twin pregnancies was significantly higher among patients with both mild GT (5.1%, $P = 8.12\times10^{-18}$) and severe GT (9.3%, $P = 2.17\times10^{-20}$) when compared to controls (3.3%), which is consistent with previous reports[1]. The median gestational age at delivery was consistent across the three groups, at 276 days (39+3 weeks). Additionally, pregnant women with GT had a higher rate of cesarean section deliveries in comparison to pregnancies in the control group (mild GT: $P = 2.23\times10^{-4}$, severe GT: $P = 2.65\times10^{-7}$). Notably, the risk of postpartum hemorrhage was 2.03 and 3.71 times higher in mild GT and severe GT cases compared to controls ($P = 3.12\times10^{-8}$ and $P = 3.20\times10^{-5}$, respectively), in line with previous studies[2,3]. A lower proportion of spontaneous preterm birth and stillbirth were observed among pregnant women with mild GT (2.4%, $P = 5.04\times10^{-8}$; 0.4%, $P = 0.032$). It should be noted that these unexpected observations may be attributable to relatively smaller sample sizes for both of these pathological pregnancy outcomes. Neonatal birth length and weight in pregnancies with mild GT were slightly higher than in the control group (both $P < 2.2\times10^{-16}$), which may be attributed to potential confounding factors.

Platelet counts change during pregnancy in GT pregnancies with platelet count measurements at all five periods

We conducted a sensitivity analysis where we focused on 14,712 pregnancies from the two hospital cohorts who had platelet count measurements at all five periods. The tendency of changes in mean platelet count is similar to the primary analysis, exhibiting a gradual decrease throughout gestation, reaching the lowest at delivery, and subsequently recovering during the postpartum period (**Figure S18 and Table S24**). Furthermore, pregnancies diagnosed with GT had a larger declining percentage and a faster mean decline rate of platelet count compared with controls (**Table S3B**), which increased with the severity of GT and maximized among the severe GT group ($P = 0.001$ and $P = 0.001$).

Changes in individual platelet count

To investigate the changes in individual platelet count, we used an R package traj (https://cran.r-project.org/web/packages/traj/index.html) to describe individual changes in platelet count. It is based on a three-step procedure proposed by Leffondree et al.[4] to cluster individual longitudinal trajectories. We chose pregnant women who had platelet count measurements at all five periods and conducted the following analysis separately in the control, mild GT, and severe GT groups: (1) computing 24 measures of change to describe the individual longitudinal trajectories; (2) performing a factor analysis for the 24 measures to select the most relevant measures; (3) performing a cluster analysis to classify individuals into different clusters according to the measures selected from step 2. The measures selected from Step 2 for each group are presented in **Table S25**. We set the number of clusters as 3. To illustrate individual changes in platelet count, we also randomly sampled 10 individuals from each cluster.

Table S25. The measures best captured the main features of the trajectories of platelet count in the 5 periods in different pregnant women group

Group	Measures of changes
Severe GT	Change (the difference between the last and the first *y*), SD of the first differences, Ratio of the mean absolute second difference to the mean absolute first difference
Mild GT	Change relative to the mean-over-time, Mean of the absolute first differences, Ratio of the mean absolute second difference to the mean absolute first difference
Control	Mean-over-time, Change relative to the mean-over-time, Maximum of the absolute first differences, Ratio of the mean absolute second difference to the mean absolute first difference

As shown in **Figure S19**, pregnancies in Cluster 1 experienced a sharp decrease in platelet count during pregnancy and recovered to nearly the level of the first trimester during the postpartum period; the platelet count of pregnancies in Cluster 2 dropped dramatically during pregnancy but moderately increased during the postpartum period; and the platelet count of pregnancies in Cluster 3 were in little change during the whole pregnancy and postpartum period. All three clusters showed the tendency for platelet count to constantly decline during pregnancy but recover after delivery. To illustrate individual changes in platelet count, we also randomly sampled 10 individuals from each cluster **(Figure S19)**.

Phenotypic analysis and genome-wide association studies on mean platelet volume (MPV) during pregnancy, at delivery and during the postpartum period

To further understand if *PEAR1* may be related to platelet activation, we conducted an additional phenotypic and GWAS analysis with MPV during the five periods as a larger MPV is attributed to an increased platelet turnover[5] and is associated with increased platelet activation[6].

Consistent with previous research findings[7,8], we observed an inverse correlation between mean platelet volume (MPV) and platelet count. The MPV of all pregnant women increased throughout pregnancy and decreased after delivery (**Figure S20**).

We further conducted GWAS for MPV at the first, second, and third trimesters during pregnancy among 71,605 Chinese pregnant women, and identified 138 independent genome-wide

significant loci (187 signals) (**Figure S21; Table S25**). GWAS for MPV at delivery and postpartum revealed 39 loci (46 signals) and 82 loci (89 signals), respectively.

We also identified two loci of MPV with time-dependent genetic effects. Interestingly, one of these loci is in the *PEAR1* locus (**Figure S22A; Table S12**). The genetic effect (absolute value) of rs12041331-A allele on MPV from the first trimester to the third trimester experiences a notable increase (3.91-fold). This trend aligns with the findings from the analysis of platelet count.

The TrajGWAS outcomes evaluating genetic variants affecting the mean of MPV across pregnancies coincided with the trimester-specific MPV GWAS results (**Figure S23A, C; Table S26 and S27**). Notably, SNPs associated with MPV changes during pregnancy, demonstrated consistent and significant associations within the *PEAR1* locus at 1q23.1 across both hospital cohorts (**Figure S24A, C; Table S28 and S29**). The lead SNP rs12566888-G allele in each cohort (Longgang: β=0.19, τ = 0.08340, $P = 4.19 \times 10^{-9}$ and Baoan: β=0.19, τ = 0.0836, $P = 3.68 \times 10^{-10}$) was associated with a faster increase in MPV throughout pregnancy and the postpartum period.

Supplementary Methods

Study population

Between 2017 and 2022, a total of 121,687 Chinese pregnant women who participated in a pregnancy screening program at two hospital cohorts in Shenzhen, China, were enrolled in our study. The Longgang cohort consists of 70,739 pregnancies from Longgang District Maternity and Child Healthcare Hospital of Shenzhen City. The Baoan cohort consists of 50,948 pregnancies from Shenzhen Baoan Women's and Children's Hospital. To ensure sample accuracy, we excluded 5,625 pregnancies potentially involving multiple gestations during the study period, as well as 15,947 pregnancies for which platelet count results were unavailable.

The research design is summarized in **Figure 1**, and the characteristics of the participants are presented in **Table S1**.

This study was approved by the Medical Ethics Committee of the School of Public Health (Shenzhen), Sun Yat-sen University, Longgang District Maternity and Child Healthcare Hospital

of Shenzhen City, and Shenzhen Baoan Women's and Children's Hospital. Data collection was approved by the Human Genetic Resources Administration of China (HGRAC).

Phenotype definition

In the GWAS analyzing platelet count throughout the first, second, and third trimesters, we selected the earliest platelet count measurement within each trimester. Platelet count at delivery was determined by considering platelet count results within 24 hours prior to delivery. If multiple platelet count measurements were available at delivery and during the postpartum period, the mean platelet count was calculated.

As for GWAS of GT, to eliminate thrombocytopenia caused by other conditions, pregnancies with preeclampsia, HELLP syndrome (hemolysis, elevated liver enzymes, and low platelet count), primary immune thrombocytopenia, HIV infection, hepatitis B virus, and hepatitis C virus infection were excluded from both the GT cases and controls. As GT typically does not lead to severe thrombocytopenia[9,10], pregnant women with one or more platelet counts less than 50×10^9/L during pregnancy were also excluded. According to the inclusion and exclusion criteria, 6,839 and 5,230 pregnancies were excluded for GT and severe GT, respectively, and we obtained 11,138 GT cases and 85,294 controls, 906 severe GT cases and 97,283 controls.

Imputation

Imputation of autosomal chromosomes and the X chromosome for the two hospital cohorts was carried out using GLIMPSE (version 1.1.1) with default parameters according to the GLIMPSE tutorial documentation[11]. The reference panel utilized was from the Born in Guangzhou Cohort Study (BIGCS) (http://gdbig.bigcs.com.cn/), resulting in 12,910,816 bi-allelic SNPs with a MAF $\geqslant$ 0.001.

Variant annotation

Variant annotation was conducted using Ensembl Variant Effect Predictor (VEP)[12] (version 101), with indexed GRCh38 cache files (version 109). HGVS notations were generated by primary

assembled reference FASTA files for *Homo sapiens*. All of these data used for annotation were pre-downloaded from the Ensembl FTP server (https://ftp.ensembl.org/pub/). As a variant may overlap multiple transcripts, we used --pick options to assign one block of consequence for each variant based on a set of VEP default criteria. The --nearest option was used to identify the nearest gene with a protein-coding transcription start site (TSS) for variants located in the intergenic region.

Statistical analyses

We used the Kruskal-Wallis test to compare age, BMI, SBP, and DBP of the first trimester, gestation age at delivery, newborn birth length and birth weight, and Chi-squared test or Fisher's exact test to compare mode of conception, mode of delivery, the proportion of fetal sex, twin pregnancy, spontaneous preterm birth and stillbirth among controls, mild GT cases, and severe GT cases. The Jonckheere-Terpstra test was conducted with the R package clinfun (version 1.1.1) (https://cran.r-project.org/web/packages/clinfun/index.html). The linear mixed model was implemented using the R package lmerTest[13] (version 3.1-3) (https://cran.r-project.org/web/packages/lmerTest/index.html).

LD score regression

The linkage disequilibrium (LD) score intercepts and λ_{GC} were calculated using the LD score (LDSC[14]) regression to distinguish inflation between polygenicity and confounding bias. We also conducted LDSC[15] regression to estimate SNP-based heritability and genetic correlations (r_g) between 5 quantitative traits (platelet count during the first, second, and third trimesters, at delivery, and during the postpartum period) and 2 qualitative traits (GT and severe GT).

Selection of proxy SNPs to conduct external replication

If our lead SNP was not present in the BBJ GWAS summary statistics, a proxy SNP in the BBJ data with LD $R^2 > 0.8$ was used as a substitute. Proxy SNPs were queried using the LDproxy Tool through LDlink[16] 5.5.1 release (11/15/2022) based on GRCh37 1000G genome build in CHB and CHS populations.

Identification of novel locus and signal

We downloaded all associations (v1.0.2_e109_r2023-02-15) from GWAS Catalog[17] to identify novel associated SNPs. Novel locus was defined as no SNPs reported to be associated with platelet count in the GWAS Catalog within the ±500kb block of the SNP. If there were variants reported as associated with platelet count in the GWAS Catalog within ±500kb of the SNP, and the LD R^2 between the SNP and the previously reported variant was less than 0.2, this SNP was defined as a novel signal.

The LD R^2 between the genome-wide significant independent SNP in our studies and variants reported in GWAS Catalog was calculated using the LDpair Tool through LDlink[16] 5.5.1 release (11/15/2022) based on GRCh38 1000G genome build in the EAS and EUR populations.

Co-localization analysis

For GWAS of platelet counts in BBJ, we selected the same region of SNPs as of pregnant women (the ±500kb block of lead SNPs), and only SNPs in these two GWAS summary statistics were included in co-localization analyses. We set the prior probability of an SNP associated with platelet counts of pregnant women (p_1) and in BBJ (p_2) as 1×10^{-4}, and the prior probability of an SNP associated with both traits (p_{12}) as 5×10^{-6} [18]. We defined a locus successfully co-localized when the posterior probability that both traits are associated and share a single causal variant (PPH4) ≥ 0.8. We also extracted a 95% credible set of each locus with accumulated SNP $PPH_4 \geq$ 0.95.

TrajGWAS analyses

TrajGWAS[19] is a recently developed method based on a mixed-effects location scale model, which can implement GWAS of longitudinal biomarkers and identify variants that contribute to mean or within-subject variability of biomarkers. Ko et al. interpreted within-subject variability as fluctuation of the biomarker for an individual around its mean.

According to the pipeline described by Ko et al.[19], we first conducted the score test across all of the SNPs with MAF ≥ 0.01 and obtained the direction of effect (β or τ) and *P* values affecting the mean and within-subject variability of platelet count. Then we performed the Wald test on the SNPs with *P* values less than 5×10^{-8} to estimate the effect size.

TrajGWAS analyses were carried out with a Julia package TrajGWAS.jl[19] (https://github.com/OpenMendel/TrajGWAS.jl). Manhattan plots and QQ plots in **Supplementary Figures 7 and 8** were plotted using a Julia package MendelPlots.jl[20] (https://github.com/OpenMendel/MendelPlots.jl).

We used PLINK[21] (version 1.9) (www.cog-genomics.org/plink/1.9/) --clump to identify independent significant loci. Variants within 1Mb from the lead SNP and with LD R^2 larger than 0.01 were divided into one clump.

Polygenic risk score

An independent NIPT PLUS pregnancy cohort was used to train the polygenic risk scores (PRSs) model of platelet counts during the first, second, and third trimesters. Between 2020 and 2021, 5,733 pregnant women who participated in the pregnancy screening program from Shenzhen Baoan Women's and Children's Hospital were recruited, all received Non-Invasive Prenatal Testing (NIPT) and provided written informed consent. These participants are characterized by a deeper sequencing depth in comparison to conventional NIPT. The genotyping and quality control processes of NIPT PLUS cohort participants were the same as Baoan and Longgang. 4,642 pregnant women with at least one platelet count testing result were included in the following derivation and validation of PRSs.

We used our meta-analysis of GWAS summary statistics for platelet counts of the first, second, and third trimesters during pregnancy (base GWAS data) to obtain the effect size of association SNPs. The PRSs were derived in NIPT PLUS (target data). The target data was randomly divided into the training (80%) and testing sets (20%). To obtain robust model estimates, we implemented a 10-fold cross-validation in the training set. The original training set was randomly divided into 10 subgroups, one subgroup was set as a validation set (10%) and the remaining 9 subgroups were set

as a new training set (90%). The new training set was used to derive PRSs. We evaluated the performance of the PRS of each period during pregnancy on the platelet count of the corresponding period by linear regression in the validation set. After changing the validation set in turn and repeating the process 9 times, we selected the optimal PRS (with the highest explained phenotypic variance (R^2)) and reported the threshold of *P* value. We then performed linear regression on platelet count using the optimal PRS in the testing set and reported adjusted-R^2 of PRS and Spearman rank correlation coefficient (r_s). We also adjusted for the top 10th principal component, maternal age, and gestation age corresponding to the time of the platelet count measurement, and reported the r_s and adjusted-R^2 of covariate models and the combined models. Similar to the aforementioned approach, we also constructed the optimal PRS for GT. To assess the ability of (1) the optimal PRS of GT, (2) the optimal PRS of platelet count during the first, second, and third trimesters, (3) the optimal PRS of GT combined with the three optimal PRSs of platelet count, (4) the optimal PRS of GT combined with the three optimal PRSs of platelet count and covariates to predict GT, we performed logistic regression in the testing set of GT and reported the C-statistics of the receiver operating characteristic (ROC) curve and Nagelkerke R^2.

We used the genome-wide clumping and thresholding (C+T) method implemented in PRSice-2[22] to construct PRSs for platelet counts of the 5 periods during pregnancy and GT. The distance for clumping was set within ±500kb of lead SNP, and the threshold of LD R^2 was 0.2. The LD R^2 was calculated on our reference panel BIGCS. The *P*-value threshold was systematically varied, commencing at 5×10^{-8} and incremented by 5×10^{-5} in each step, until reaching the values of 0.5 and 1, in order to ascertain the optimal P-value threshold.

Reference:

1. Fogerty AE, Dzik W. Gestational thrombocytopenia: a case-control study of over 3,500 pregnancies. *Br J Haematol*. 2021;194(2):433-438.
2. Carlson LM, Dotters-Katz SK, Smid MC, Manuck TA. How Low Is Too Low? Postpartum Hemorrhage Risk among Women with Thrombocytopenia. *Am J Perinatol*. 2017;34(11):1135-1141.
3. Govindappagari S, Moyle K, Burwick RM. Mild Thrombocytopenia and Postpartum Hemorrhage in Nulliparous Women With Term, Singleton, Vertex Deliveries. *Obstet Gynecol*. 2020;135(6):1338-1344.
4. Leffondré K, Abrahamowicz M, Regeasse A, et al. Statistical measures were proposed for identifying longitudinal patterns of change in quantitative health indicators. *J Clin Epidemiol*. 2004;57(10):1049-1062.
5. Martin JF, Trowbridge EA, Salmon G, Plumb J. The biological significance of platelet volume: its relationship to bleeding time, platelet thromboxane B2 production and megakaryocyte nuclear DNA concentration. *Thromb Res*. 1983;32(5):443-460.
6. Tsiara S, Elisaf M, Jagroop IA, Mikhailidis DP. Platelets as predictors of vascular risk: is there a practical index of platelet activity? *Clin Appl Thromb Hemost*. 2003;9(3):177-190.
7. Thompson C, Jakubowski J. The pathophysiology and clinical relevance of platelet heterogeneity. *Blood*. 1988;72(1):1-8.
8. Tygart SG, McRoyan DK, Spinnato JA, McRoyan CJ, Kitay DZ. Longitudinal study of platelet indices during normal pregnancy. *Am J Obstet Gynecol*. 1986;154(4):883-887.
9. ACOG Practice Bulletin No. 207: Thrombocytopenia in Pregnancy. *Obstet Gynecol*. 2019;133(3):e181-e193.
10. Cines DB, Levine LD. Thrombocytopenia in pregnancy. *Blood*. 2017;130(21):2271-2277.
11. Rubinacci S, Ribeiro DM, Hofmeister RJ, Delaneau O. Efficient phasing and imputation of low-coverage sequencing data using large reference panels. *Nat Genet*. 2021;53(1):120-126.
12. McLaren W, Gil L, Hunt SE, et al. The Ensembl Variant Effect Predictor. *Genome Biol*. 2016;17(1):122.
13. Kuznetsova A, Brockhoff PB, Christensen RH. lmerTest package: tests in linear mixed effects models. *Journal of statistical software*. 2017;82:1-26.
14. Bulik-Sullivan BK, Loh PR, Finucane HK, et al. LD Score regression distinguishes confounding from polygenicity in genome-wide association studies. *Nat Genet*. 2015;47(3):291-295.
15. Bulik-Sullivan B, Finucane HK, Anttila V, et al. An atlas of genetic correlations across human diseases and traits. *Nat Genet*. 2015;47(11):1236-1241.
16. Machiela MJ, Chanock SJ. LDlink: a web-based application for exploring population-specific haplotype structure and linking correlated alleles of possible functional variants. *Bioinformatics*. 2015;31(21):3555-3557.
17. Buniello A, MacArthur JAL, Cerezo M, et al. The NHGRI-EBI GWAS Catalog of published genome-wide association studies, targeted arrays and summary statistics 2019. *Nucleic Acids Res*. 2019;47(D1):D1005-d1012.
18. Wallace C. Eliciting priors and relaxing the single causal variant assumption in colocalisation analyses. *PLoS Genet*. 2020;16(4):e1008720.
19. Ko S, German CA, Jensen A, et al. GWAS of longitudinal trajectories at biobank scale. *Am J Hum*

Genet. 2022;109(3):433-445.
20. Zhou H, Sinsheimer JS, Bates DM, et al. OPENMENDEL: a cooperative programming project for statistical genetics. *Hum Genet*. 2020;139(1):61-71.
21. Chang CC, Chow CC, Tellier LC, Vattikuti S, Purcell SM, Lee JJ. Second-generation PLINK: rising to the challenge of larger and richer datasets. *Gigascience*. 2015;4:7.
22. Choi SW, O'Reilly PF. PRSice-2: Polygenic Risk Score software for biobank-scale data. *Gigascience*. 2019;8(7).

Supplementary Table Legends

Table S1. Demographic and clinical characteristics of mild GT cases, severe GT cases, and controls during pregnancy

Table S2. The parameter estimation and variance analysis results of Linear Mixed Effects Model 1.

Table S3. Supplementary Table 3. Comparison of the declining percentage and the mean decline rate of platelet count from the first trimester to the time of delivery.

Table S4. The parameter estimation and variance analysis results of Linear Mixed Effects Model 2.

Table S5. SNP-based heritability and LD score regression results of platelet count during the first, second, and third trimesters, at delivery, and during the postpartum period.

Table S6. Genetic correlations between platelet count during the first, second, and third trimesters, at delivery, and during the postpartum period.

Table S7. Genome-wide significant signals of meta-analyses and GWASs of platelet counts during the first, second, and third trimesters, at delivery, and during the postpartum period in two cohorts.

Table S8. GWAS meta-analyses results for platelet count and MPV during the first, second, and third trimesters, at delivery, and during the postpartum period, and GT.

Table S9. 8 novel genome-wide significant loci of GWAS meta-analyses of platelet counts during the first, second, and third trimesters, at delivery, and the postpartum period.

Table S10. Successfully colocalized (Posterior probability of colocalization ≥ 0.8) and the highest probability variant implicated by colocalization.

Table S11. Lead SNPs with time-dependent genetic effects of platelet count and MPV during the first, second, and third trimesters.

Table S12. Meta-analysis results of all SNPs with time-dependent genetic effects during the first, second, and third trimesters.

Table S13. The parameter estimation of the null model of TrajGWAS analysis for Longgang.

Table S14. The parameter estimation of the null model of TrajGWAS analysis for Baoan.

Table S15. Lead SNPs associated with the mean of platelet count for Longgang.

Table S16. Lead SNPs associated with the mean of platelet count for Baoan.

Table S17. All variants associated with within-subject (WS) variability of platelet count during pregnancy for Longgang.

Table S18. All variants associated with within-subject (WS) variability of platelet count during pregnancy for Baoan.

Table S19. Genome-wide significant signals of GWAS meta-analysis for GT.

Table S20. The optimal platelet count polygenic risk scores and their performance in validation sets.

Table S21. The performance of the optimal platelet count polygenic risk scores in testing sets.

Table S22. The performance of the optimal platelet count polygenic risk scores for predicting GT.

Table S23. Maternal and neonatal outcomes of mild GT cases, severe GT cases, and controls during pregnancy.

Table S24. Demographic characteristics and platelet count of mild GT cases, severe GT cases, and controls of pregnancies with platelet count measurements at all five periods.

Table S25. Genome-wide significant signals of meta-analyses and GWASs of MPV during the first, second, and third trimesters, at delivery, and during the postpartum period in two cohorts.

Table S26. Lead SNPs associated with mean of MPV for Longgang

Table S27. Lead SNPs associated with mean of MPV for Baoan

Table S28. All variants associated with within-subject (WS) variability of MPV during pregnancy for Longgang

Table S29. All variants associated with within-subject (WS) variability of MPV during pregnancy for Baoan

Supplementary Figures

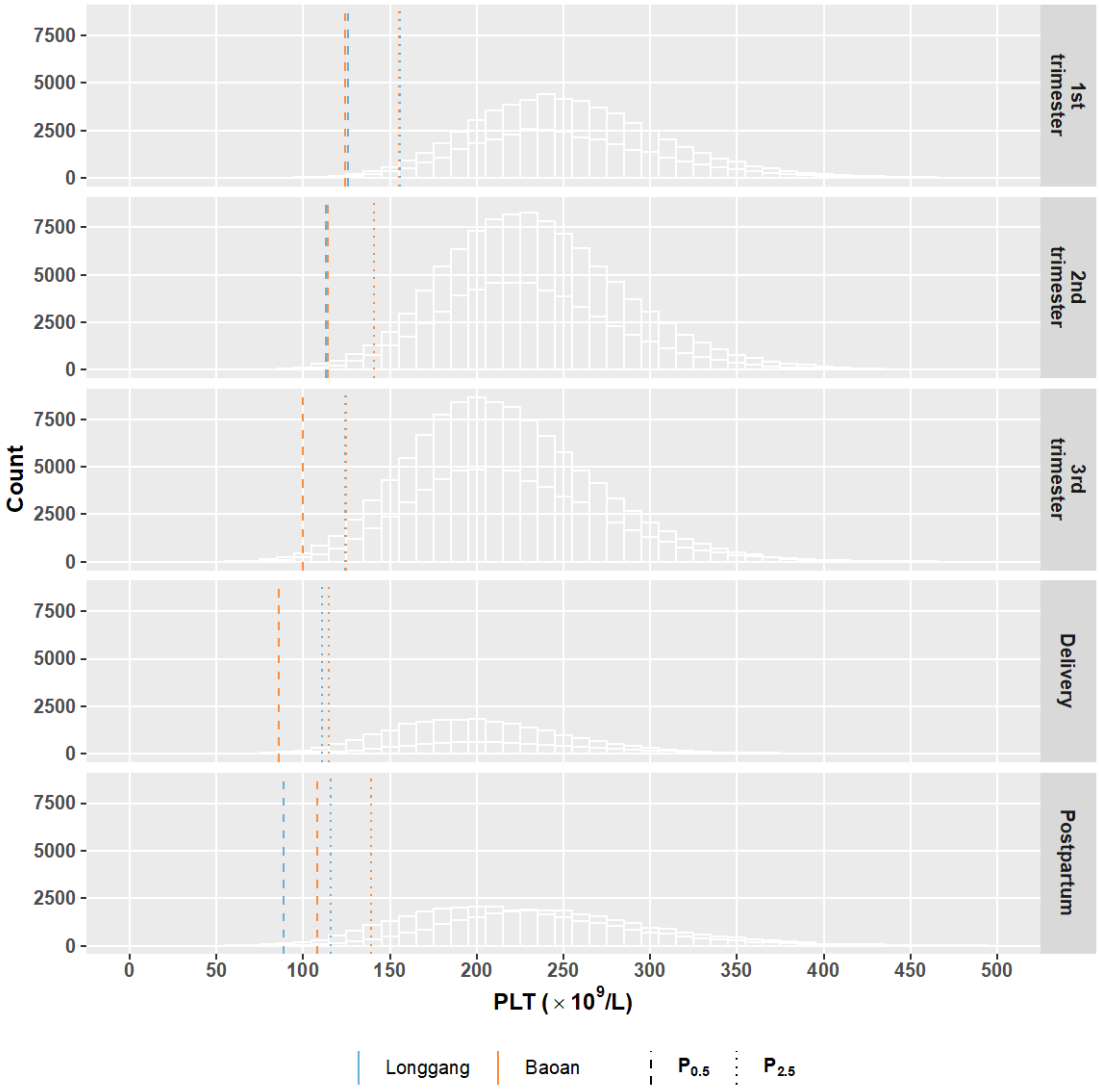

Figure S1. The distribution of platelet counts and the 0.5th and 2.5th percentiles during the first, second, and third trimesters, at delivery, and during the postpartum period from two cohorts.

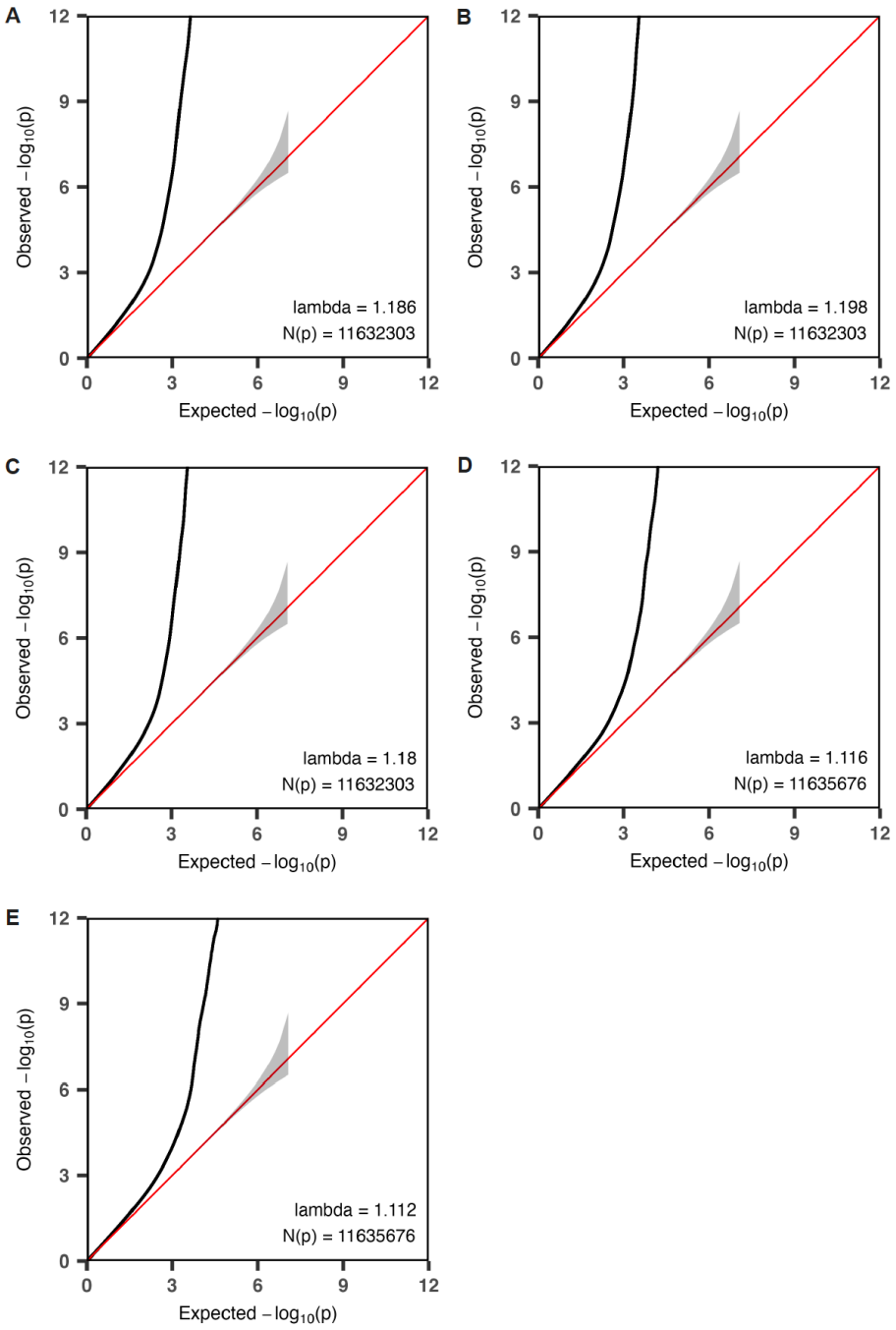

376 **Figure S2. QQ plots of GWAS meta-analyses of platelet count during pregnancy, at delivery,**
377 **and during the postpartum period.**

378 QQ plots for GWAS meta-analyses of platelet counts during (A) the first, (B) second, and (C)
379 third trimester, (D) at delivery, and (E) during the postpartum period show the observed -$\log_{10}$(*P*-
380 value) in our GWAS meta-analyses against expected -$\log_{10}$(*P*-value). The red line indicates the
381 distribution of *P* values under the null hypothesis and the gray shaded area indicates standard
382 errors.

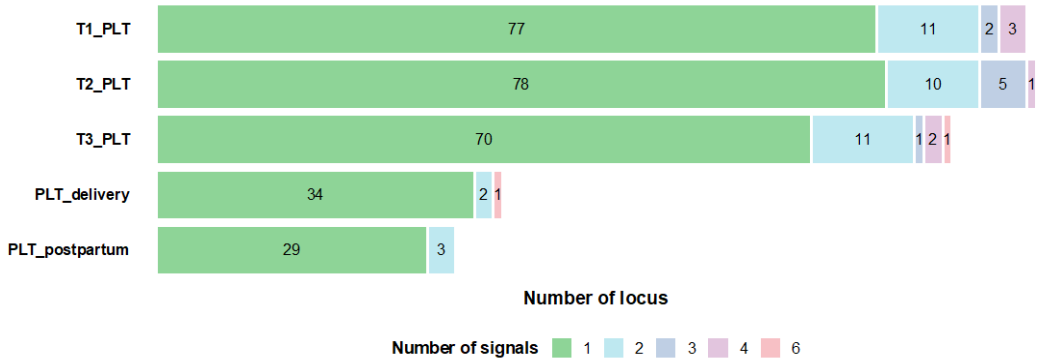

Figure S3. The number of genome-wide significant loci and signals for the GWAS meta-analyses of platelet count during pregnancy, at delivery, and during the postpartum period. The number of loci with different numbers of signals for each period is shown in the plot. T1_PLT: Platelet counts during the first trimester; T2_PLT: Platelet counts during the second trimester; T3_PLT: Platelet counts during the third trimester; PLT_delivery: Platelet counts at delivery; PLT_postpartum: Platelet counts during the postpartum period.

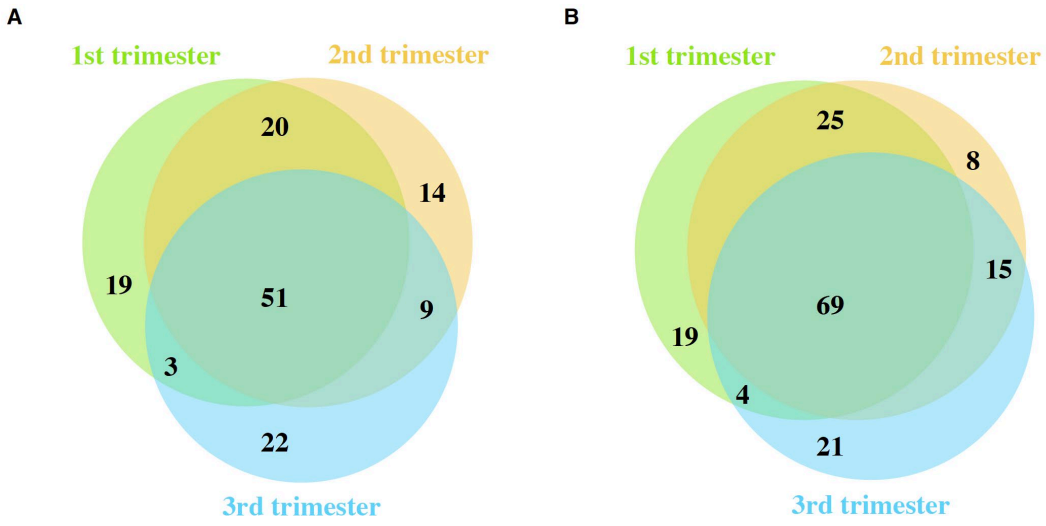

Figure S4. The number of genome-wide significant loci and signals for platelet count during the first, second, and third trimesters.

Venn diagrams showing the number of genome-wide significant (A) loci and (B) signals for platelet count during the first, second, and third trimesters. The number of unique loci/signals for each trimester and shared loci/signals between or among different trimesters are shown in the corresponding regions.

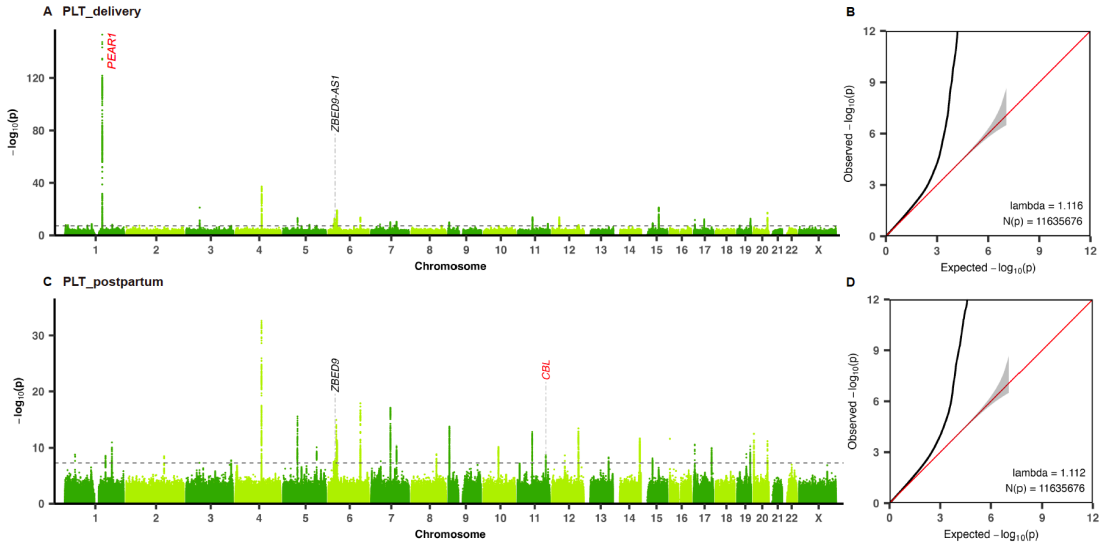

Figure S5. Manhattan plots and QQ plots for GWAS of platelet count at delivery and during the postpartum period.

GWASs of platelet count at delivery and during the postpartum period were undertaken with 33,553 and 34,457 Chinese pregnant women, respectively. Manhattan plots for GWAS meta-analyses of platelet counts (A) at delivery and (C) during the postpartum period. GWAS for each hospital was carried out with a linear regression model, and the first to tenth principal components, maternal age, and gestation age correspond to the time of the platelet count test as covariates. The x-axis shows the ordered chromosomes and the y-axis indicates -$\log_{10}$(*P*-value) for the association tests. The dashed black line represents the genome-wide significance threshold for GWAS ($P = 5\times10^{-8}$). A total of 37 and 32 genome-wide significant independent loci (44 and 35 signals) achieved the genome-wide significance threshold. Labels in black indicate the novel loci, and labels in red highlight the two loci (*PEAR1* and *CBL*) with time-dependent genetic effects during pregnancy. QQ plots for GWAS meta-analyses of platelet counts (B) at delivery and (D) during the postpartum period show the observed -$\log_{10}$(*P*-value) in our GWAS meta-analyses against expected -$\log_{10}$(*P*-value). The red dashed line indicates the distribution of *P* values under the null hypothesis and the gray shaded area indicates standard errors.

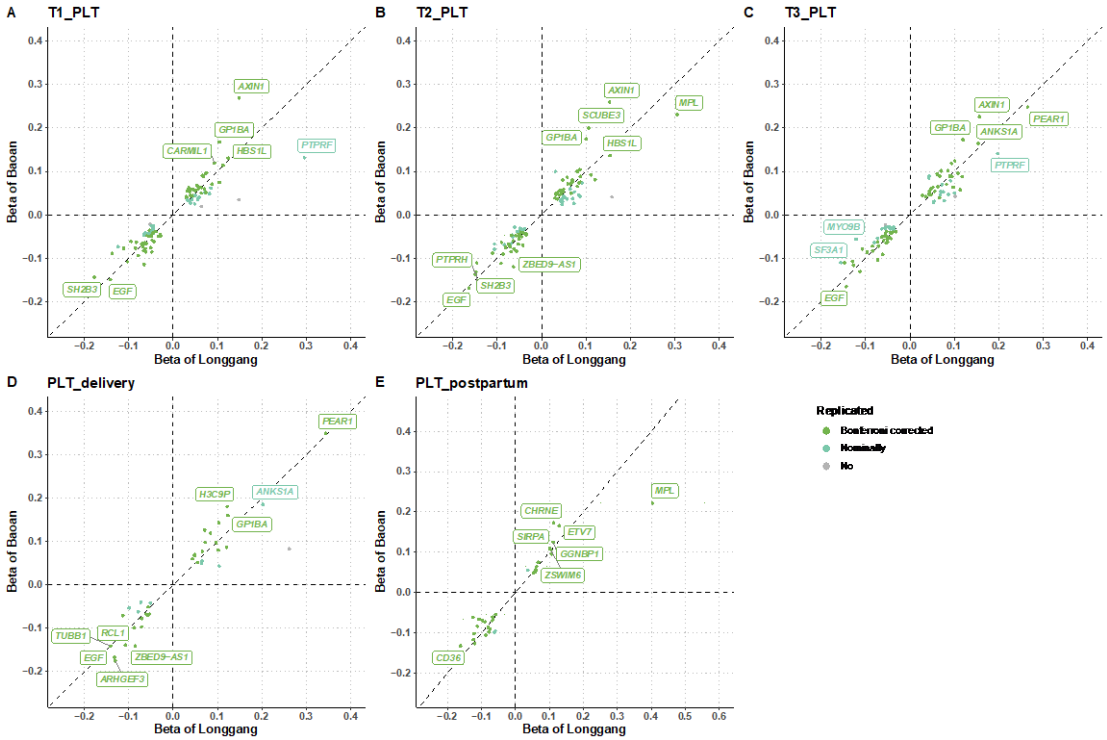

Figure S6. Comparing GWAS of platelet count during pregnancy, at delivery, and during the postpartum period of Longgang to Baoan.

Comparing the direction of beta and *P* values of the lead SNPs of GWAS of platelet count during (A) the first trimester, (B) the second trimester, (C) the third trimester, (D) at delivery, and (E) during the postpartum period between the two hospitals. The x-axis indicates the beta of GWAS of each trait for Longgang, and the y-axis indicates the beta of GWAS for Baoan. The error bars indicate the 95% CI of beta. Colored points represent lead SNPs with the same direction of beta and Bonferroni corrected significant *P* values (green), with the same direction of beta and nominally significant *P* values (cyan), and with different directions of beta and/or *P* values > 0.05 (grey). The Bonferroni significant threshold was calculated as 0.05 divided by the number of independent loci for each trait.

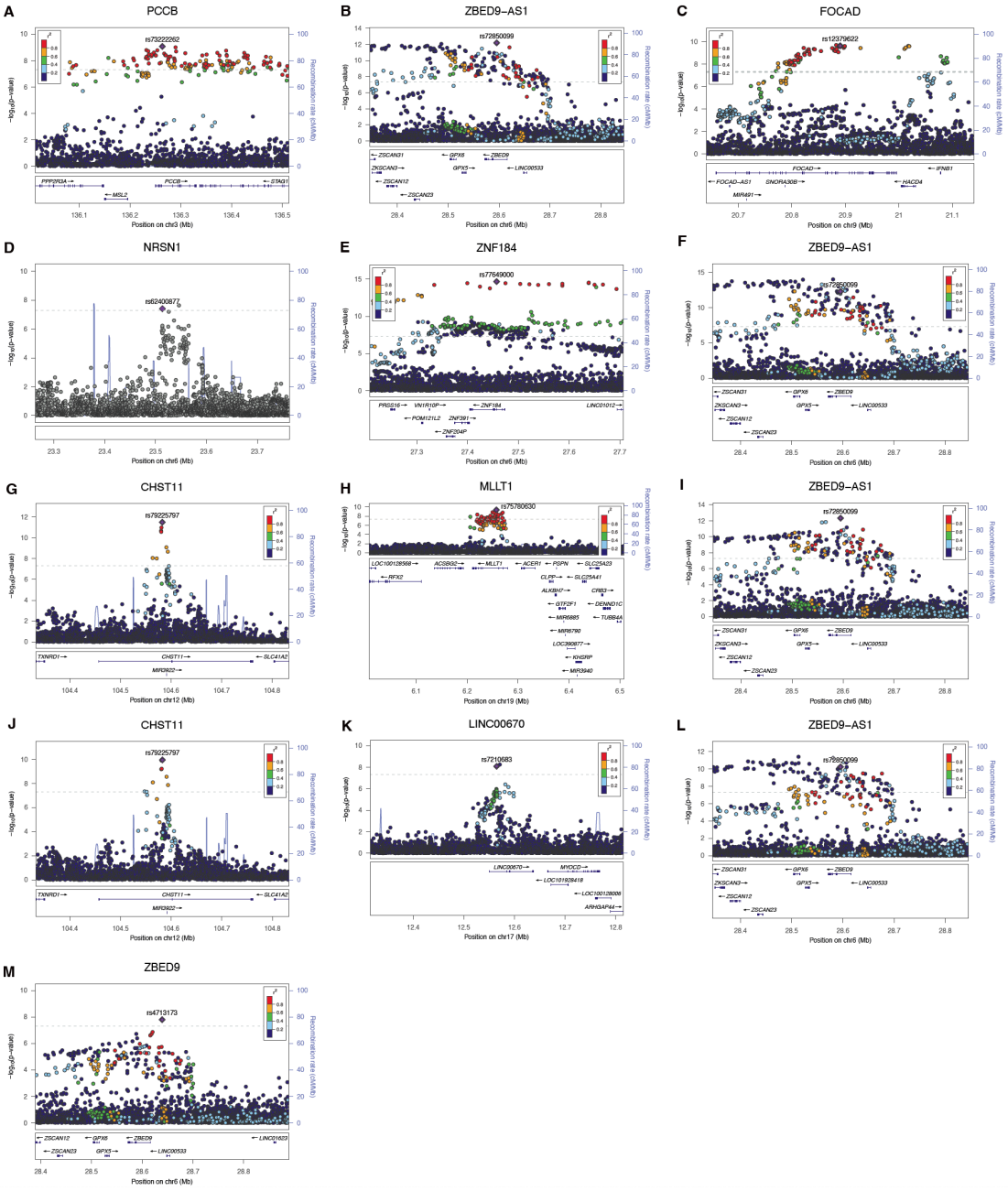

Figure S7. Regional association plots for novel loci of GWAS meta-analyses of platelet count during pregnancy, at delivery, and during the postpartum period.

Regional association plots for novel loci of GWAS meta-analyses of platelet count during the first trimester at (A) 3q22.3 (*PCCB*), (B) 6p22.1 (*ZBED9-AS1*), and (C) 9p21.3 (*FOCAD*), during the second trimester at (D) 6p22.3 (*NRSN1*), (E) 6q22.1 (*ZNF184*), (F) 6p22.1 (*ZBED9-AS1*), (G) 12q23.3 (*CHST11*), and (H) 19p13.3 (*MLLT1*), during the third trimester at (I) 6p22.1 (*ZBED9-AS1*), (J) 12q23.3 (*CHST11*), and (K) 17p12 (*LINC00670*), at delivery at (L) 6p22.1 (*ZBED9-AS1*), and during the postpartum period at (M) 6p22.1 (*ZBED9*). The *x* axis shows the

chromosomal positions (GRCh38) and the *y* axis indicates -$\log_{10}$(*P*-value) for the association tests. The purple diamond indicates the lead SNP of each locus. The other SNPs are colored based on their LD r^2 with the lead SNP. The dashed grey line represents the genome-wide significance threshold for GWAS ($P = 5\times10^{-8}$).

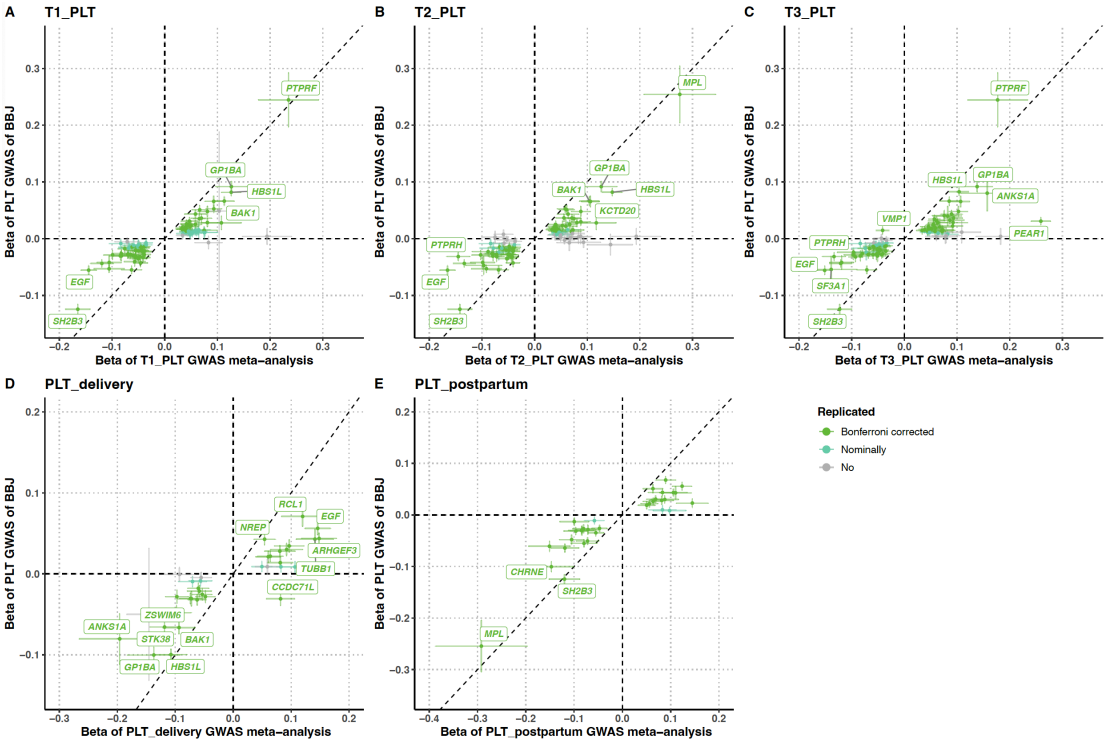

440 **Figure S8. Comparing GWAS meta-analyses of platelet count during pregnancy, at delivery,**
441 **and during the postpartum period to the GWAS summary statistics of platelet count in BBJ.**
442 Comparing the independent genome-wide significant loci of our GWAS meta-analyses during (A)
443 the first trimester, (B) the second trimester, (C) the third trimester, (D) at delivery, and (E) during
444 the postpartum period to a GWAS of platelet count from the BioBank Japan Project (BBJ). The x-
445 axis indicates the beta of GWAS of each trait in our GWAS meta-analyses, and the y-axis
446 indicates the beta of GWAS of platelet count in BBJ. The error bars indicate the 95% CI of beta.
447 Colored points represent lead SNPs with the same direction of beta and Bonferroni corrected
448 significant *P* values (green), with the same direction of beta and nominally significant *P* values
449 (cyan), and with different directions of beta and/or *P* values > 0.05 (grey). The Bonferroni
450 significant threshold was calculated as 0.05 divided by the number of independent loci for each
451 trait.
452

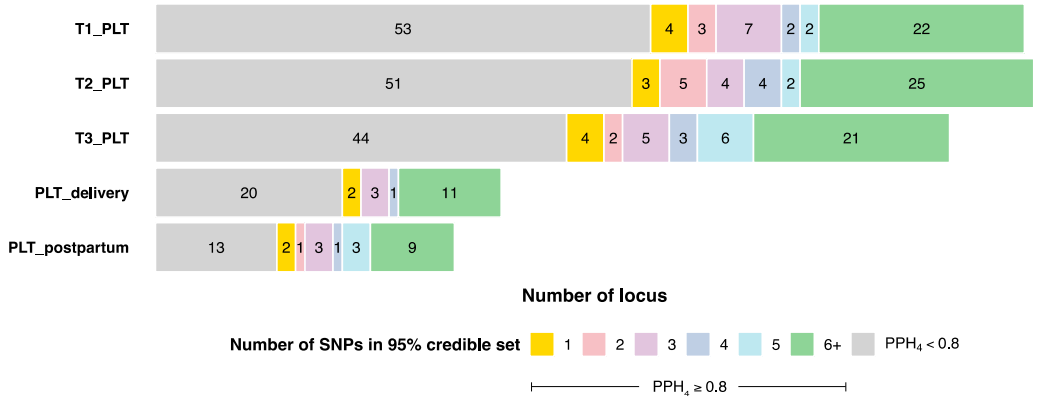

Figure S9. The result of co-localization between the GWAS of platelet count of the five periods of pregnancy and the platelet count in BBJ.

The grey bars represent the number of loci unsuccessfully co-localized ($PPH_4 < 0.8$. The bars in the other six colors represent the number of loci successfully co-localized ($PPH_4 \geqslant 0.8$), these colors represent the different numbers of SNPs (from 1 to 6+) in the 95% credible set of each locus. BBJ: the BioBank Japan Project; T1_PLT: Platelet counts during the first trimester; T2_PLT: Platelet counts during the second trimester; T3_PLT: Platelet counts during the third trimester; PLT_delivery: Platelet counts at delivery; PLT_postpartum: Platelet counts during the postpartum period.

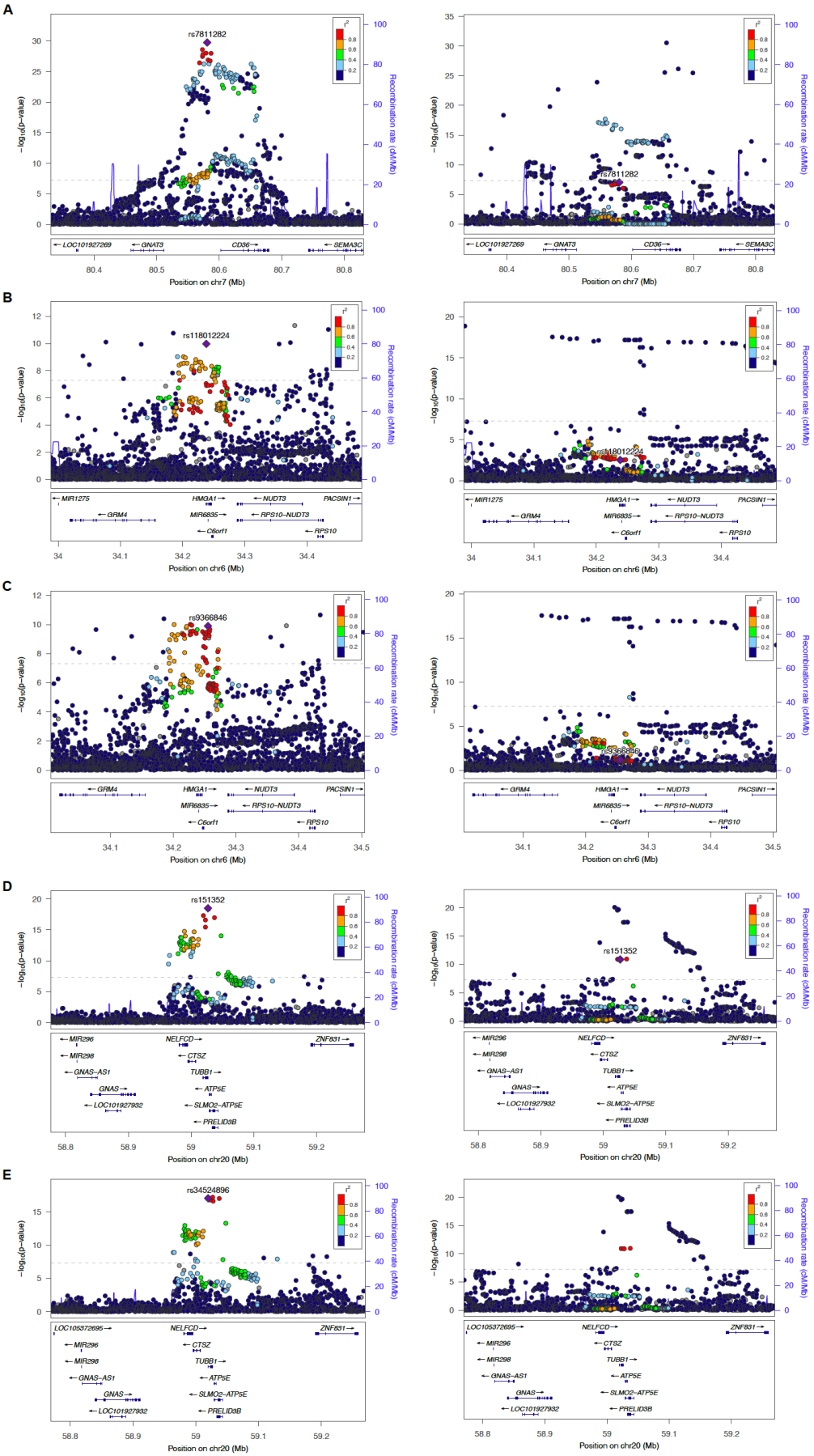
A
rs7811282
LOC101927269
GNAT3
CD36
SEMA3C
Position on chr7 (Mb)
B
rs118012224
MIR1275
HMGA1
NUDT3
PACSIN1
GRM4
MIR6835
RPS10-NUDT3
C6orf1
RPS10
Position on chr6 (Mb)
C
rs9366846
Position on chr6 (Mb)
D
rs151352
MIR296
NELFCD
ZNF831
MIR298
CTSZ
GNAS-AS1
TUBB1
GNAS
ATP5E
LOC101927932
SLMO2-ATP5E
PRELID3B
Position on chr20 (Mb)
E
rs34524896
LOC105372695
Position on chr20 (Mb)
−log10(p-value)
Recombination rate (cM/Mb)

Figure S10. Regional association plots for five loci with the smallest PPH4 values in the co-localization analysis.

The plots on the left are regional association plots of our GWAS meta-analyses of platelet count, and the plots on the right are GWAS of platelet count in BBJ. (A) Regional association plots for our GWAS meta-analyses of platelet count during the first trimester and GWAS of platelet count in BBJ at 7q21.11 (*CD36*). (B) Regional association plots for our GWAS meta-analyses of platelet count during the first trimester and GWAS of platelet count in BBJ at 6p21.31 (*HMGA1*). (C) Regional association plots for our GWAS meta-analyses of platelet count during the second trimester and GWAS of platelet count in BBJ at 6p21.31 (*SMIM29*). (D) Regional association plots for our GWAS meta-analyses of platelet count during the first trimester and GWAS of platelet count in BBJ at 20q13.32 (*ATP5F1E*). (E) Regional association plots for our GWAS meta-analyses of platelet count during the first trimester and GWAS of platelet count in BBJ at 20q13.32 (*TUBB1*). The *x* axis shows the chromosomal positions (GRCh38) and the *y* axis indicates $-\log_{10}(P\text{-value})$ for the association tests. The purple diamond indicates the lead SNP of each locus. The other SNPs are colored based on their LD r^2 with the lead SNP. The dashed grey line represents the genome-wide significance threshold for GWAS ($P = 5\times10^{-8}$).

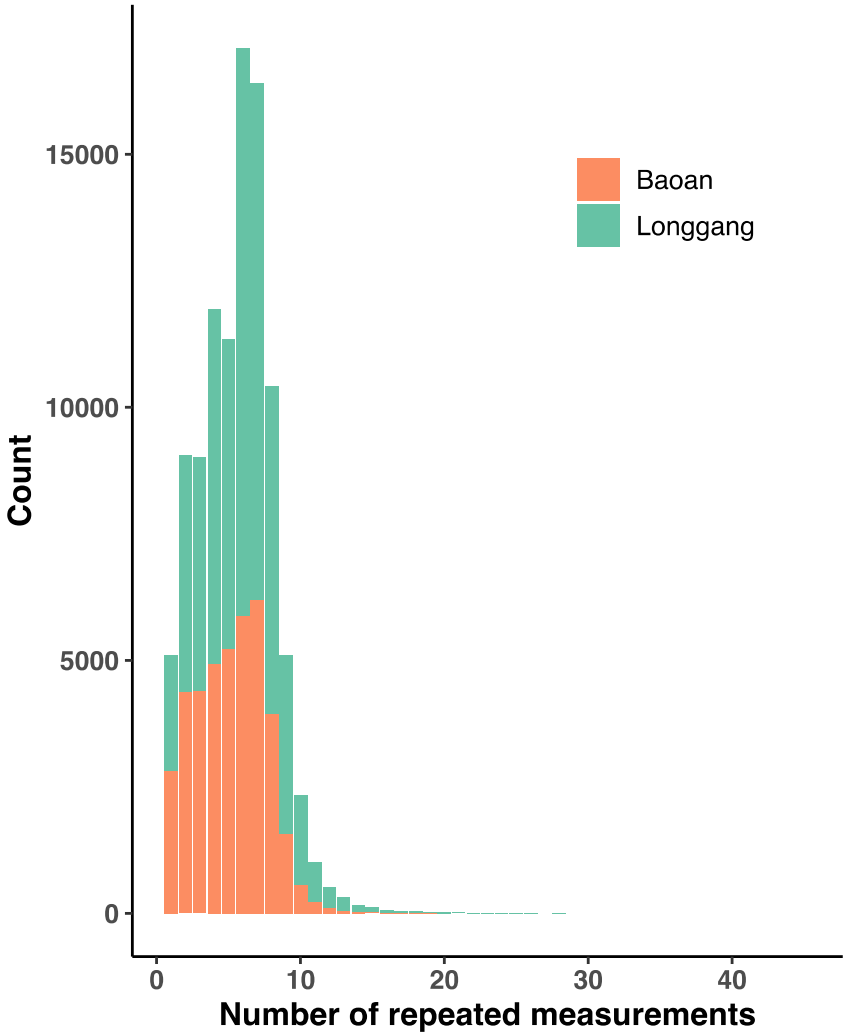

482 **Figure S11. Distribution of the number of repeated measurements of platelet counts in**

483 **Baoan and Longgang.**

484

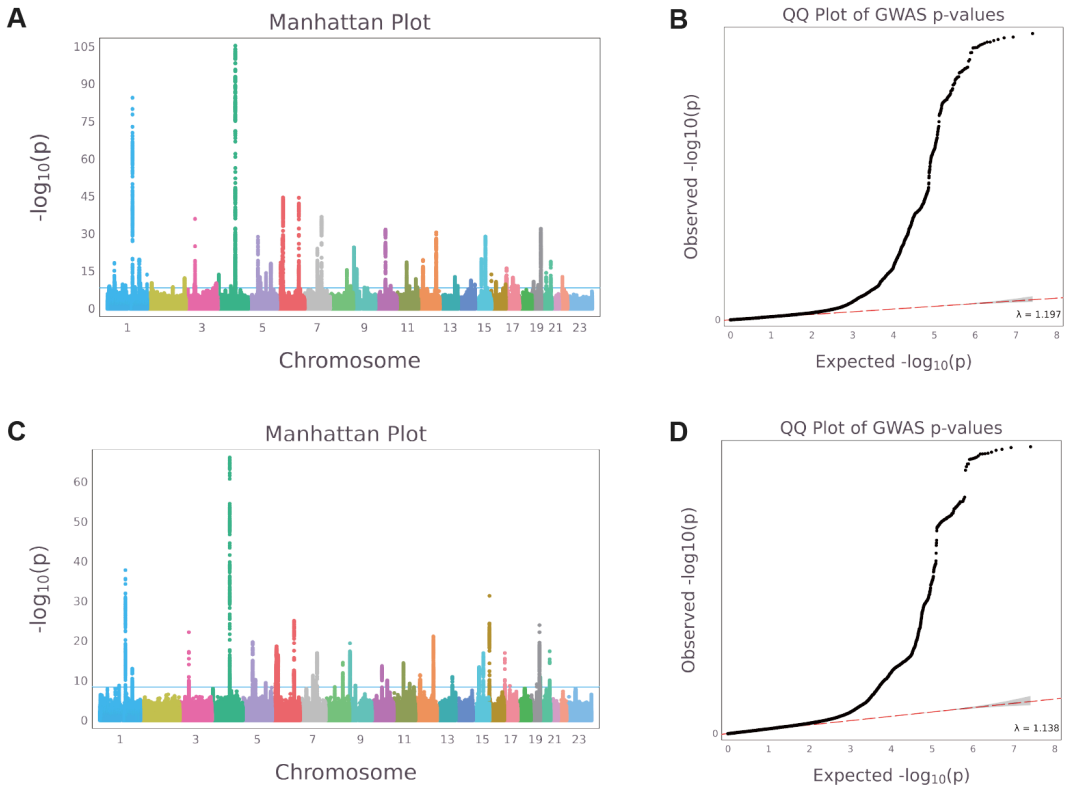

485 **Figure S12. TrajGWAS results of the mean of longitudinal platelet count during pregnancy**
486 **and the postpartum period.**

487 100,186 pregnancies (Longgang: n = 59,907, Baoan: n = 40,279) with more than one platelet
488 count during pregnancy and the postpartum period were included in the TrajGWAS analyses.
489 Platelet counts were rank-based transformed. The first to tenth principal components, age, and
490 gestation age corresponding to the time of the platelet count test were adjusted as covariates.
491 Manhattan plots for (A) Longgang and (C) Baoan. The x-axis shows the ordered chromosomes
492 and the y-axis indicates -$\log_{10}$(*P*-value) for the TrajGWAS analyses. The blue horizontal line
493 represents the genome-wide significance threshold ($P = 5\times10^{-8}$). QQ plots for (B) Longgang and
494 (D) Baoan show the observed -$\log_{10}$(*P*-value) in TrajGWAS analyses against expected -$\log_{10}$(*P*-
495 value). The red dashed line indicates the distribution of *P* values under the null hypothesis and the
496 gray shaded area indicates standard errors.
497

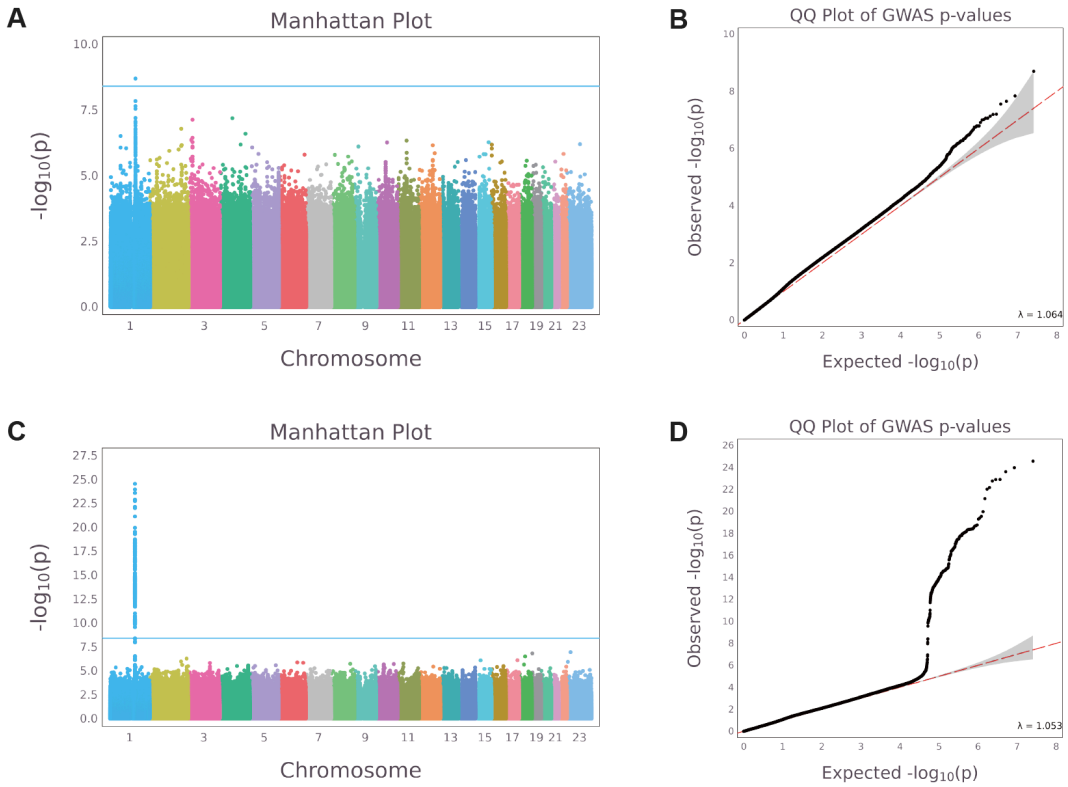

498 **Figure S13. TrajGWAS results of the within-subject variability of longitudinal platelet**
499 **counts during pregnancy and the postpartum period.**
500 100,186 pregnancies (Longgang: n = 59,907, Baoan: n = 40,279) with more than one platelet
501 count during pregnancy and the postpartum period were included in the TrajGWAS analyses.
502 Platelet counts were rank-based transformed. The first to tenth principal components, age, and
503 gestation age corresponding to the time of the platelet count test were adjusted as covariates.
504 Manhattan plots for (A) Longgang and (C) Baoan. The x-axis shows the ordered chromosomes
505 and the y-axis indicates -$\log_{10}$(*P*-value) for the TrajGWAS analyses. The blue horizontal line
506 represents the genome-wide significance threshold ($P = 5\times10^{-8}$). QQ plots for (B) Longgang and
507 (D) Baoan show the observed -$\log_{10}$(*P*-value) in TrajGWAS analyses against expected -$\log_{10}$(*P*-
508 value). The red dashed line indicates the distribution of *P* values under the null hypothesis and the
509 gray shaded area indicates standard errors.
510

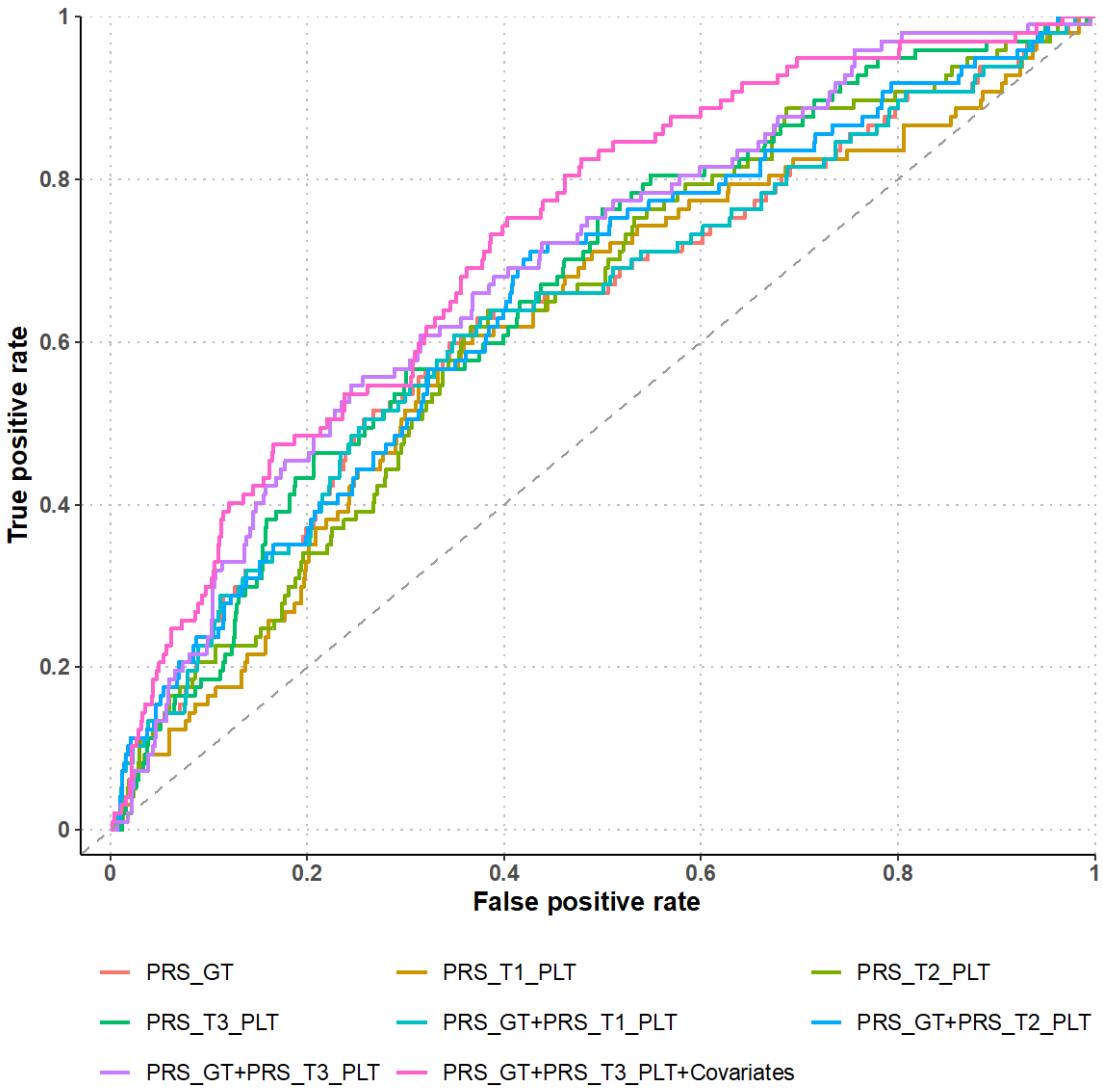

511 **Figure S14. Receiver operating characteristic (ROC) curves of 8 models for GT.**

512 Covariates include the top 10th principal component and maternal age. T1_PLT: Platelet counts
513 during the first trimester; T2_PLT: Platelet counts during the second trimester; T3_PLT: Platelet
514 counts during the third trimester; GT: Gestational Thrombocytopenia.

515

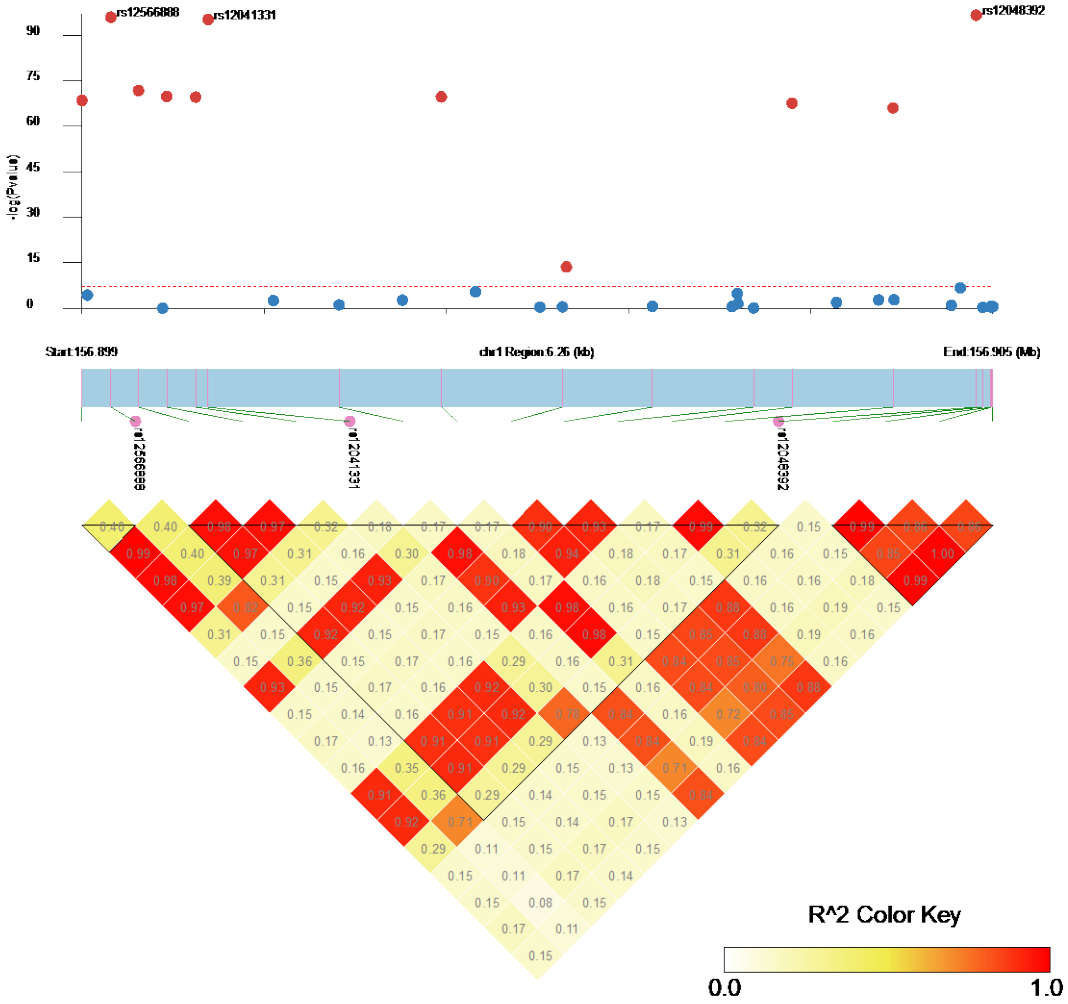

516

517 **Figure S15. Regional association plots and LD heatmap of GT in *PEAR1* locus.**

518 The LD R^2 was calculated using our reference panel from BIGCS (http://gdbig.bigcs.com.cn/).

519

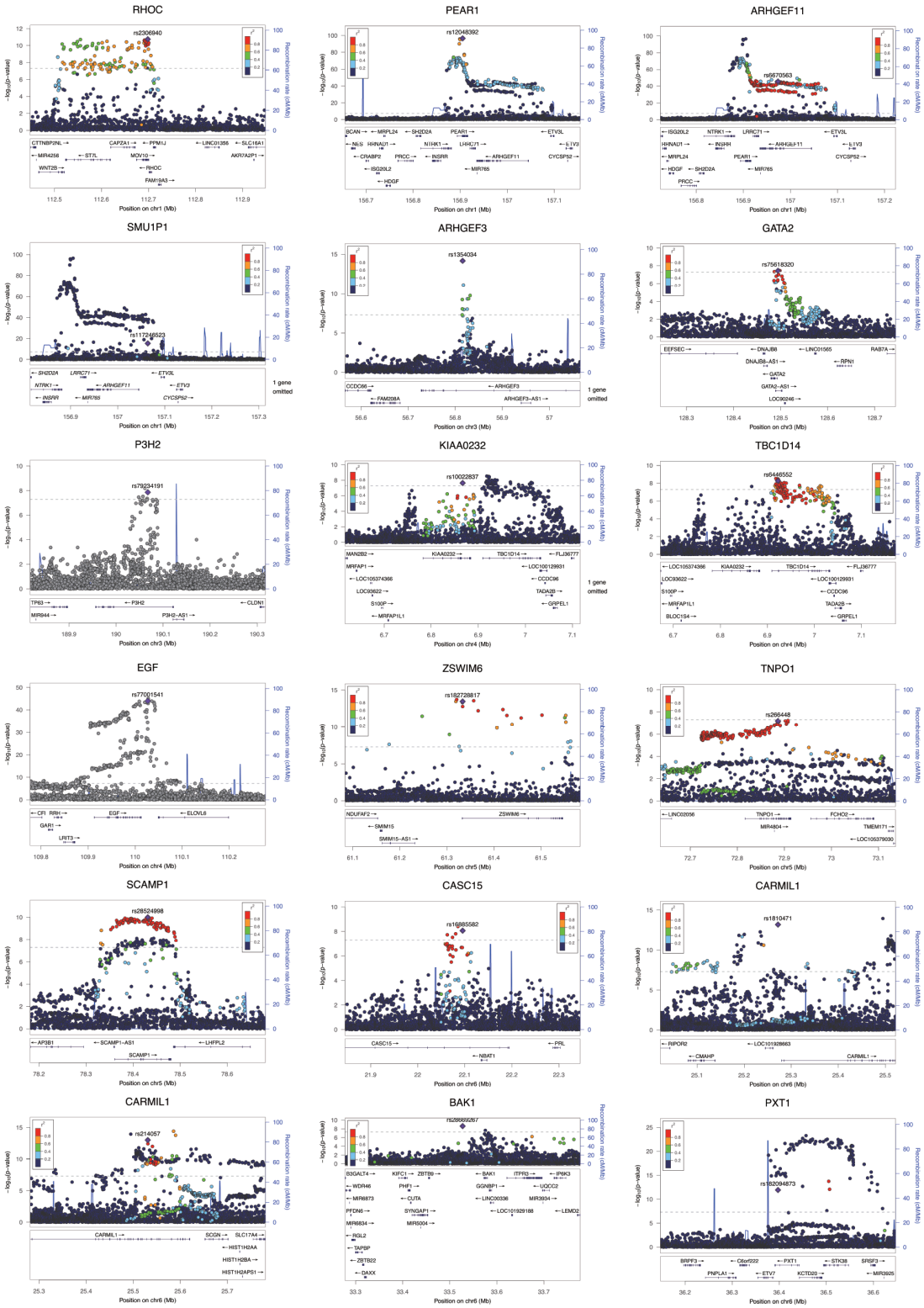
RHOC
rs2306940
PEAR1
rs12048392
ARHGEF11
rs9870563
SMU1P1
rs117248523
ARHGEF3
rs1354034
GATA2
rs75618320
P3H2
rs79234191
KIAA0232
rs10022837
TBC1D14
rs6446552
EGF
rs77001541
ZSWIM6
rs182728817
TNPO1
rs266448
SCAMP1
rs28524998
CASC15
rs16885582
CARMIL1
rs1810471
CARMIL1
rs214057
BAK1
rs528693267
PXT1
rs182094873
−log10(p-value)
Recombination rate (cM/Mb)
Position on chr1 (Mb)
Position on chr3 (Mb)
Position on chr4 (Mb)
Position on chr5 (Mb)
Position on chr6 (Mb)
1 gene omitted

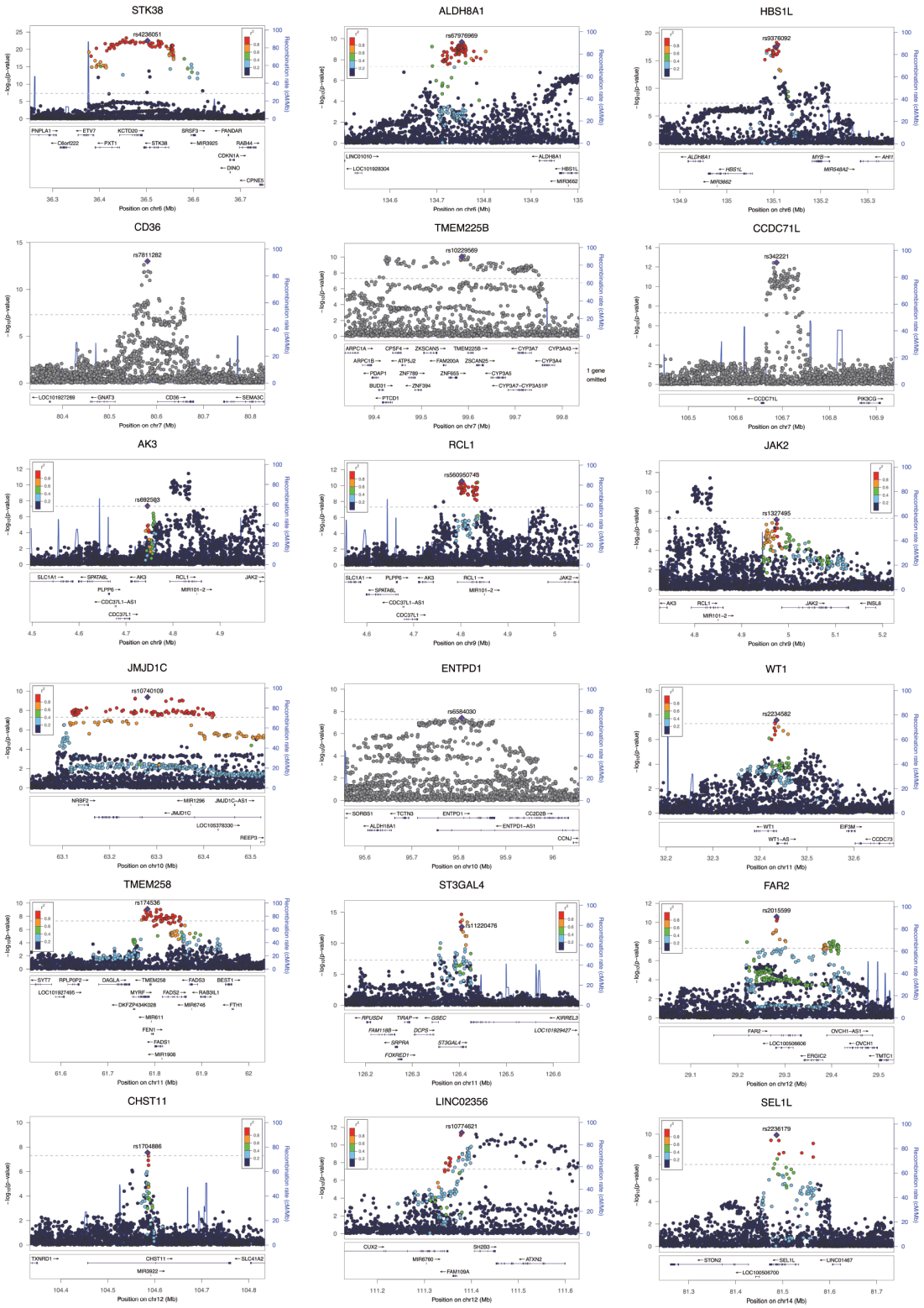
STK38
rs4236051
ALDH8A1
rs57976969
HBS1L
rs9376092
CD36
rs7811282
TMEM225B
rs10229569
1 gene omitted
CCDC71L
rs342221
AK3
rs692583
RCL1
rs560950748
JAK2
rs1327495
JMJD1C
rs10740109
ENTPD1
rs5584030
WT1
rs2234582
TMEM258
rs174536
ST3GAL4
rs11220476
FAR2
rs2015599
CHST11
rs1704886
LINC02356
rs10774621
SEL1L
rs2236179
−log10(p−value)
Recombination rate (cM/Mb)
Position on chr6 (Mb)
Position on chr7 (Mb)
Position on chr9 (Mb)
Position on chr10 (Mb)
Position on chr11 (Mb)
Position on chr12 (Mb)
Position on chr14 (Mb)

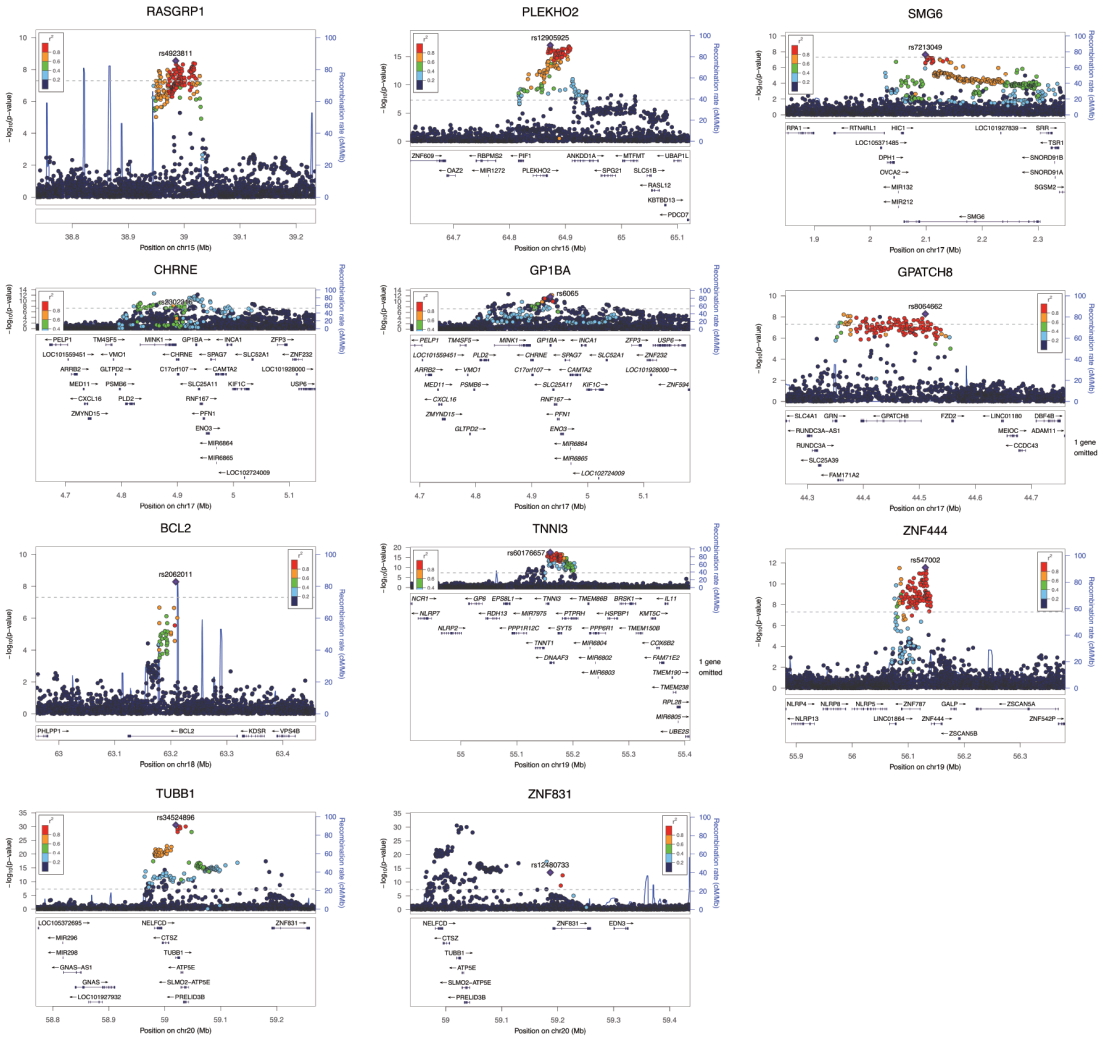

520 **Figure S16. Regional association plots for novel loci of GWAS meta-analyses of GT.**

521 Regional association plots for 37 novel loci of GWAS meta-analyses of GT. The x-axis shows the
522 chromosomal positions (GRCh38) and the y-axis indicates -$\log_{10}$(*P*-value) for the association
523 tests. The purple diamond indicates the lead SNP of each locus. The other SNPs are colored based
524 on their LD r^2 with the lead SNP. The dashed grey line represents the genome-wide significance
525 threshold for GWAS ($P = 5\times10^{-8}$).
526

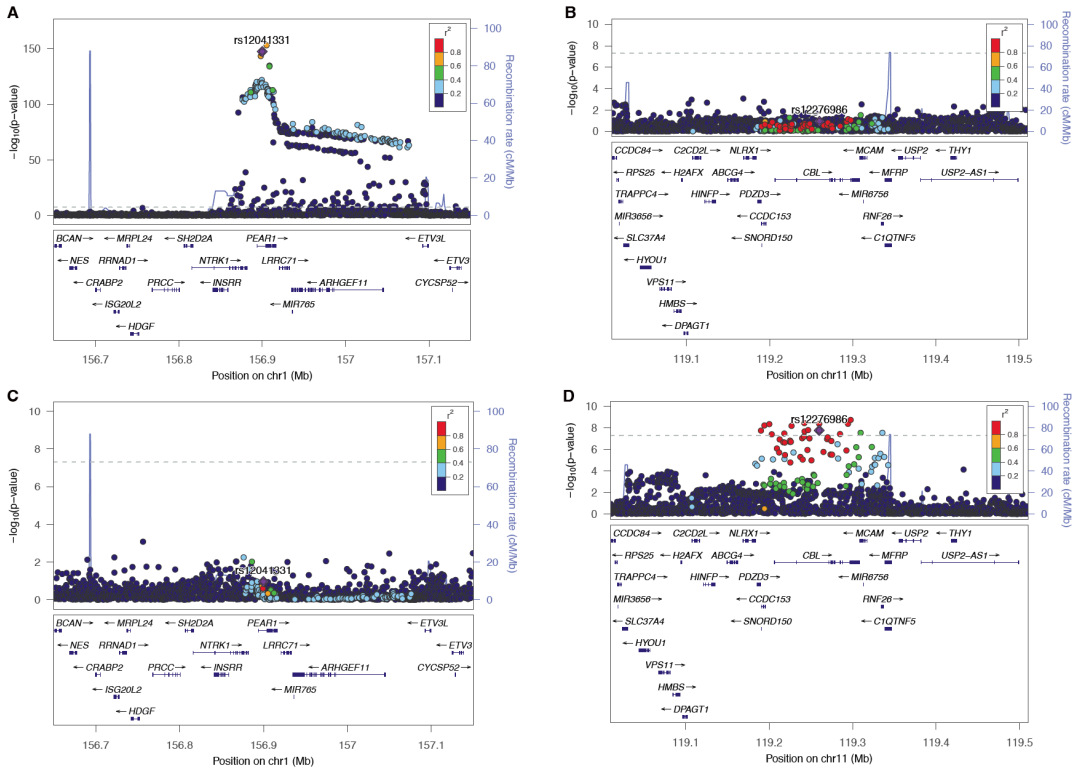

527 **Figure S17. Regional association plots of rs12041331 and rs12276986 for platelet count at**
528 **delivery and during the postpartum period.**

529 Regional association plots of rs12041331 in *PEAR1* for platelet count (A) at delivery and (C) during
530 the postpartum period, and regional association plots of rs12276986 in *CBL* for platelet count (B)
531 at delivery and (D) during the postpartum period. The x-axis shows the chromosomal positions
532 (GRCh38) and the y-axis indicates -$\log_{10}$(*P*-value) for the association tests. The purple diamond
533 indicates the lead SNP of each locus. The other SNPs are colored based on their LD r^2 with the lead
534 SNP. The dashed grey line represents the genome-wide significance threshold for GWAS ($P = 5\times10^{-8}$).
535
536

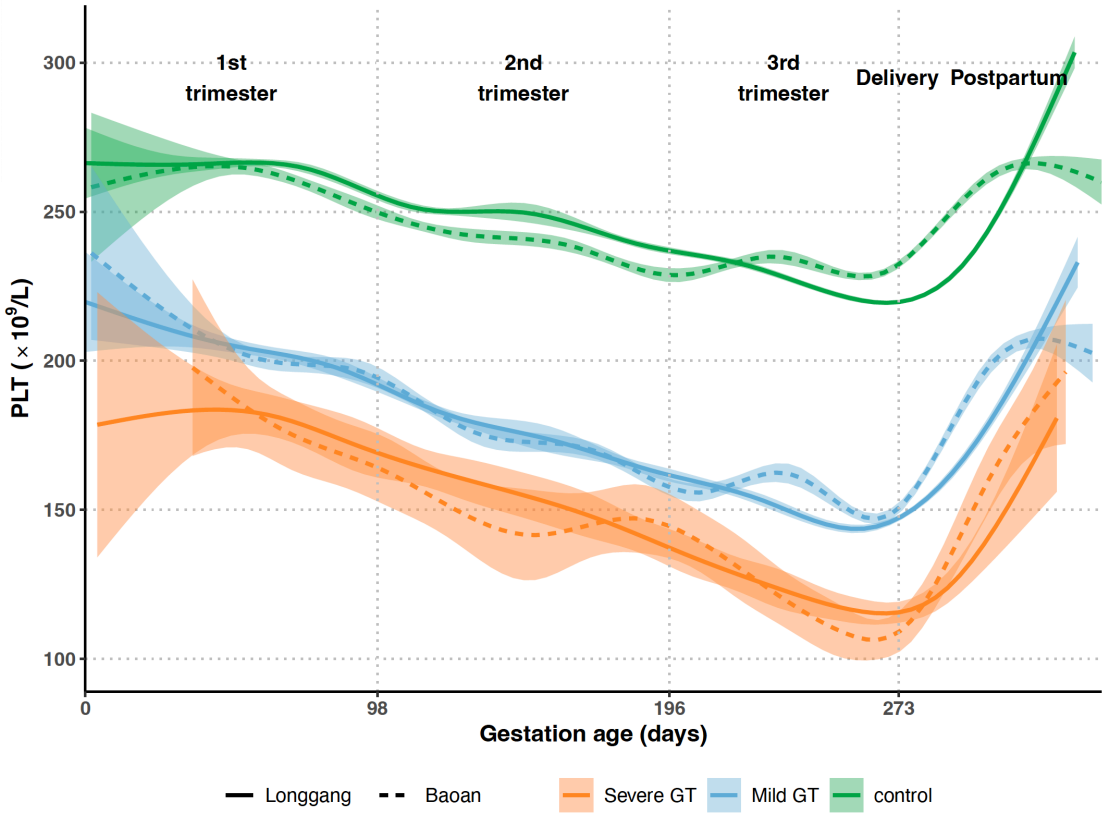

Figure S18. Mean platelet counts over gestation age.

Changes in mean platelet count during the first, second, and third trimesters, at delivery, and during the postpartum period in pregnancies diagnosed with severe GT (N = 266), mild GT (N = 1,992), and controls (N = 12,454) and with platelet count measurements at all five periods. The smoothing function is the generalized additive model. The ribbon around the smooth curve denotes the 95% confidence interval. PLT: Platelet count; GT: Gestational Thrombocytopenia; Baoan: Shenzhen Baoan Maternal and Child Health Hospital; Longgang: Longgang District Maternity and Child Healthcare Hospital of Shenzhen City.

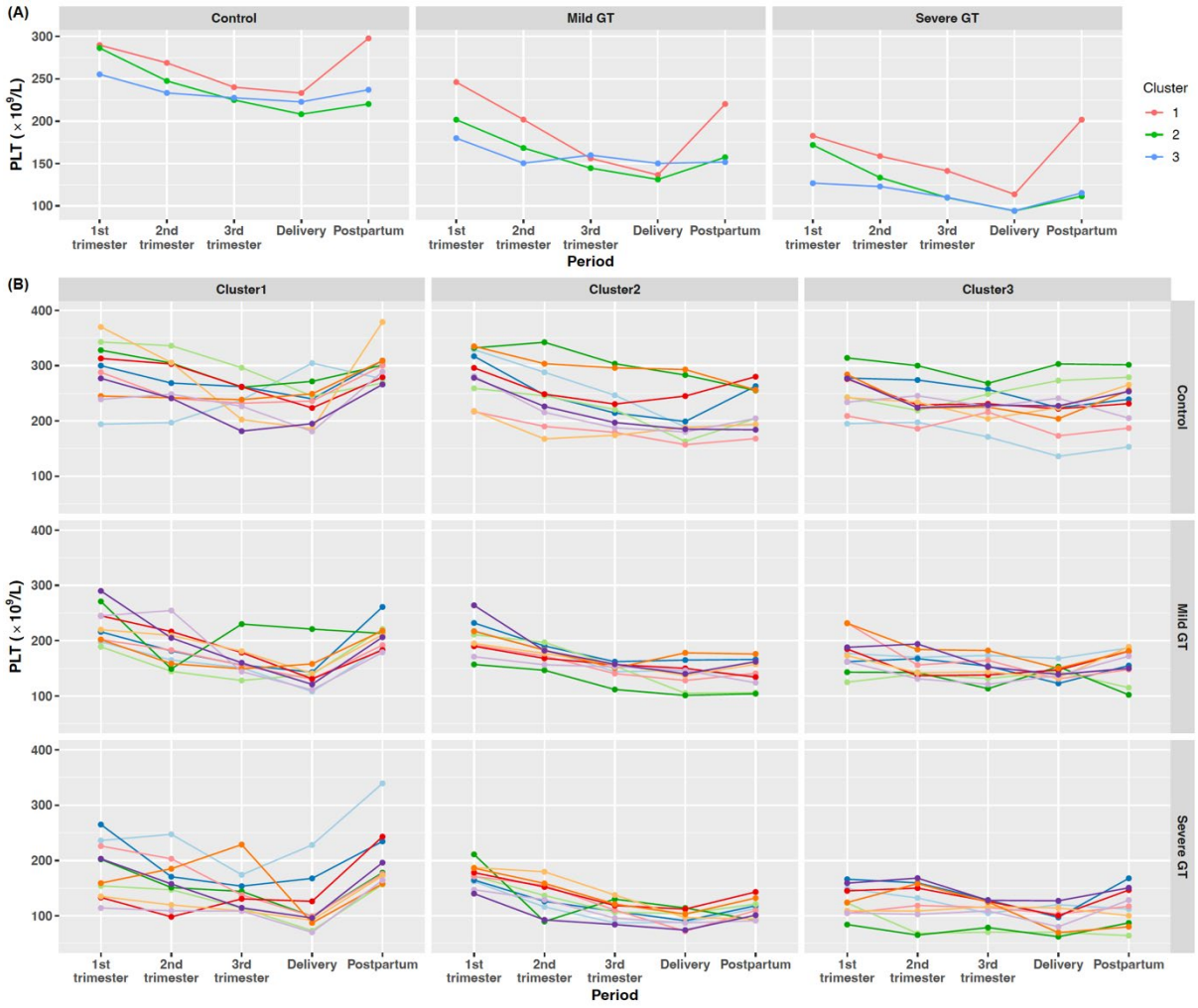

547 **Figure S19. Individual changes in platelet count among mild GT cases, severe GT cases, and**
548 **controls during pregnancy.**

549 All pregnant women with platelet count measurements at all five periods. (A) The changes of
550 mean platelet count across 5 periods in each cluster. (B) Individual changes of platelet count
551 across 5 periods (randomly sampled 10 individuals from each cluster).

552

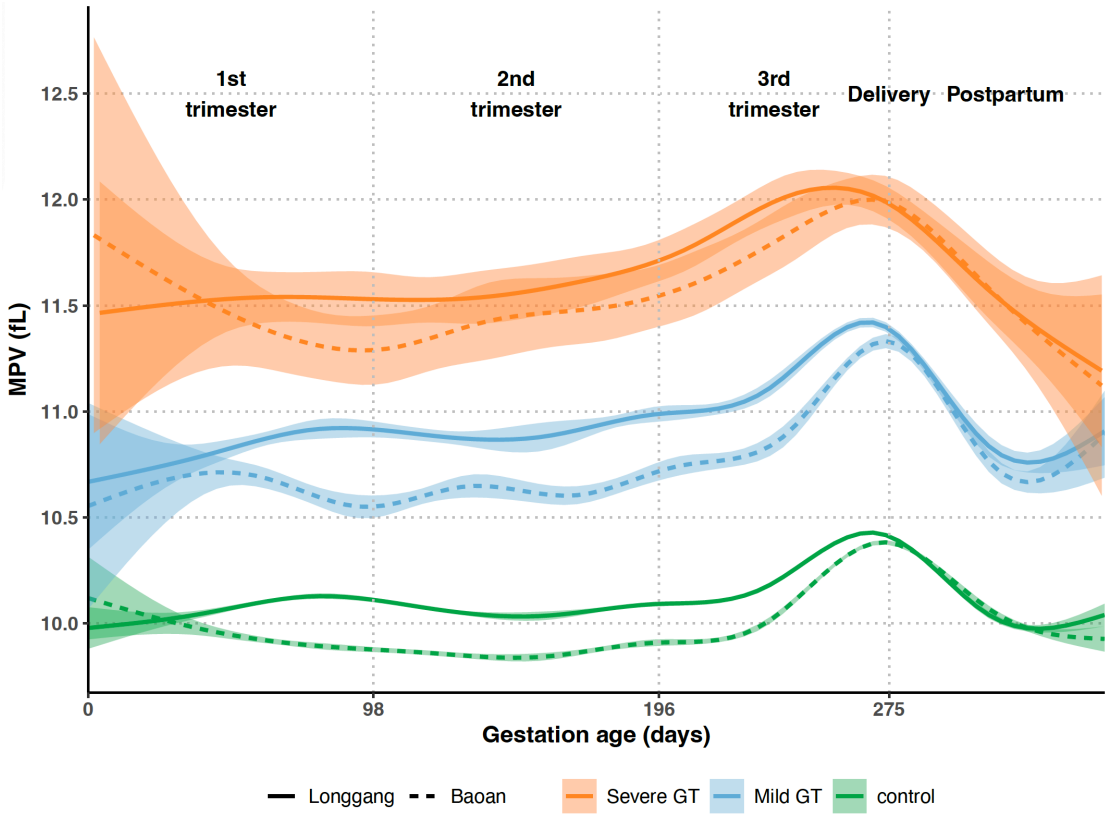

553

554 **Figure S20. Mean platelet volumes over gestation age.**

555 Changes in mean platelet volume (MPV) during the first, second, and third trimesters, at delivery,

556 and during the postpartum period in pregnancies diagnosed with severe GT (N = 859), mild GT (N

557 = 10,044), and controls (N = 83,015).

558

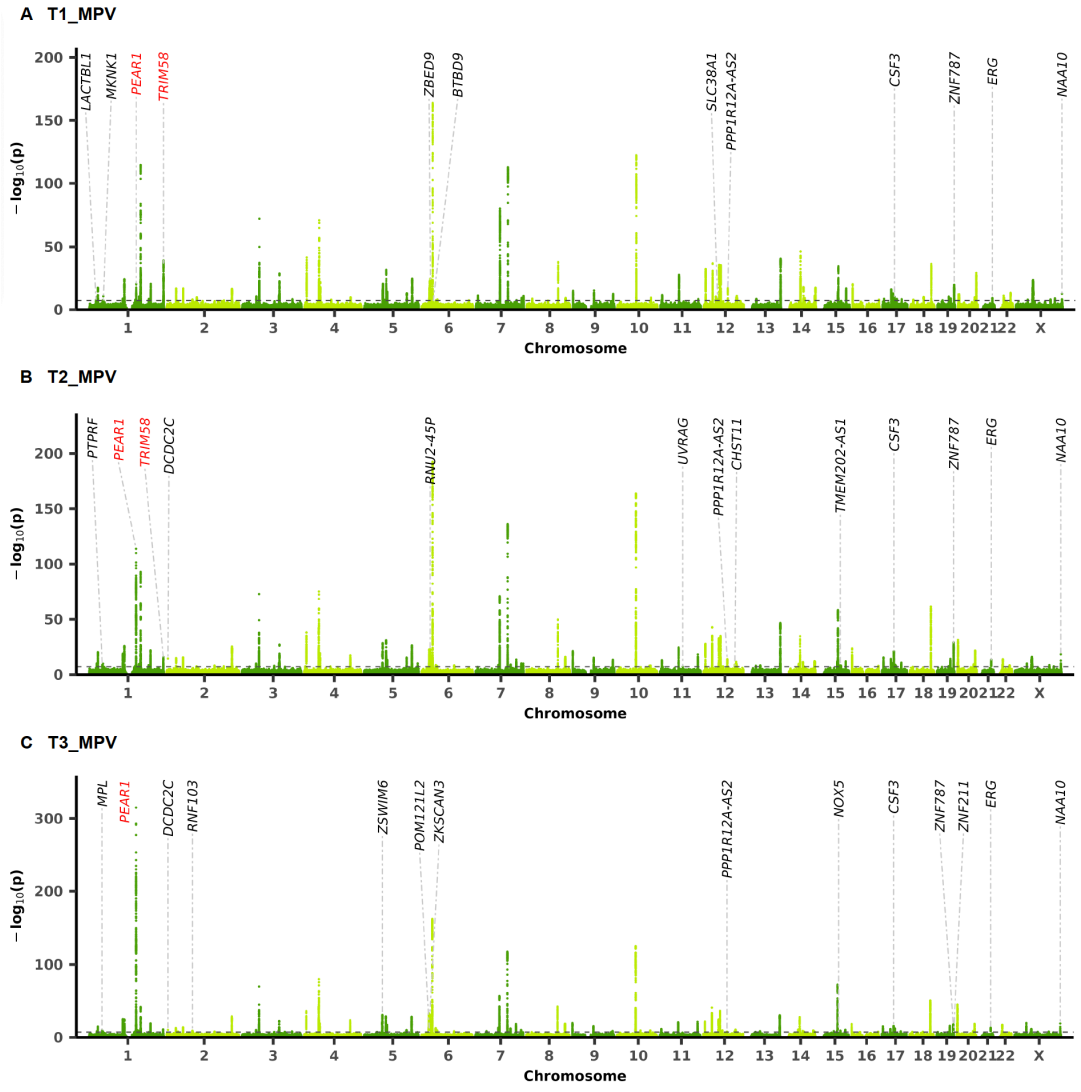
A T1_MPV
LACTBL1
MKNK1
PEAR1
TRIM58
ZBED9
BTBD9
SLC38A1
PPP1R12A-AS2
CSF3
ZNF787
ERG
NAA10
− log10(p)
Chromosome
B T2_MPV
PTPRF
PEAR1
TRIM58
DCDC2C
RNU2-45P
UVRAG
PPP1R12A-AS2
CHST11
TMEM202-AS1
CSF3
ZNF787
ERG
NAA10
− log10(p)
Chromosome
C T3_MPV
MPL
PEAR1
DCDC2C
RNF103
ZSWIM6
POM121L2
ZKSCAN3
PPP1R12A-AS2
NOX5
CSF3
ZNF787
ZNF211
ERG
NAA10
− log10(p)
Chromosome
D MPV_delivery
PEAR1
ZBED9
NAA10
− log10(p)
Chromosome
E MPV_postpartum
MKNK1
PEAR1
TRIM58
ZSWIM6
RSL24D1P1
ZBED9-AS1
UVRAG
PPP1R12A
RASGRP1
ZNF787
ERG
NAA10
− log10(p)
Chromosome

559

560

Figure S21. Manhattan plots of the genome-wide association study meta-analyses for MPV during the first, second, and third trimesters, at delivery, and during the postpartum. 71,605 Chinese pregnant women with at least one MPV in each trimester from two hospitals were included in the GWAS meta-analyses. Manhattan plots for GWAS meta-analyses of platelet counts during (A) the first trimester, (B) the second trimester, and (C) the third trimester. A total of 138 genome-wide significant independent loci (187 independent signals) achieved the genome-wide significance threshold. GWASs of platelet count (D) at delivery and (E) during the postpartum period were undertaken with 30,313 and 54,914 Chinese pregnant women, respectively. A total of 39 and 82 genome-wide significant independent loci (46 and 89 signals) achieved the genome-wide significance threshold. GWAS for each hospital was carried out with a linear regression model, and the first to tenth principal components, maternal age, and gestation age correspond to the time of the platelet count test as covariates. The x-axis shows the ordered chromosomes and the y-axis indicates -$\log_{10}$(*P*-value) for the association tests. The dashed black line represents the genome-wide significance threshold for GWAS ($P = 5 \times 10^{-8}$). Labels in black indicate the nearest gene of the novel loci, and labels in red highlight the two loci (*PEAR1* and *TRIM58*) with time-dependent genetic effects during pregnancy. T1_MPV: Mean platelet volume during the first trimester; T2_MPV: Mean platelet volume during the second trimester; T3_MPV: Mean platelet volume during the third trimester.

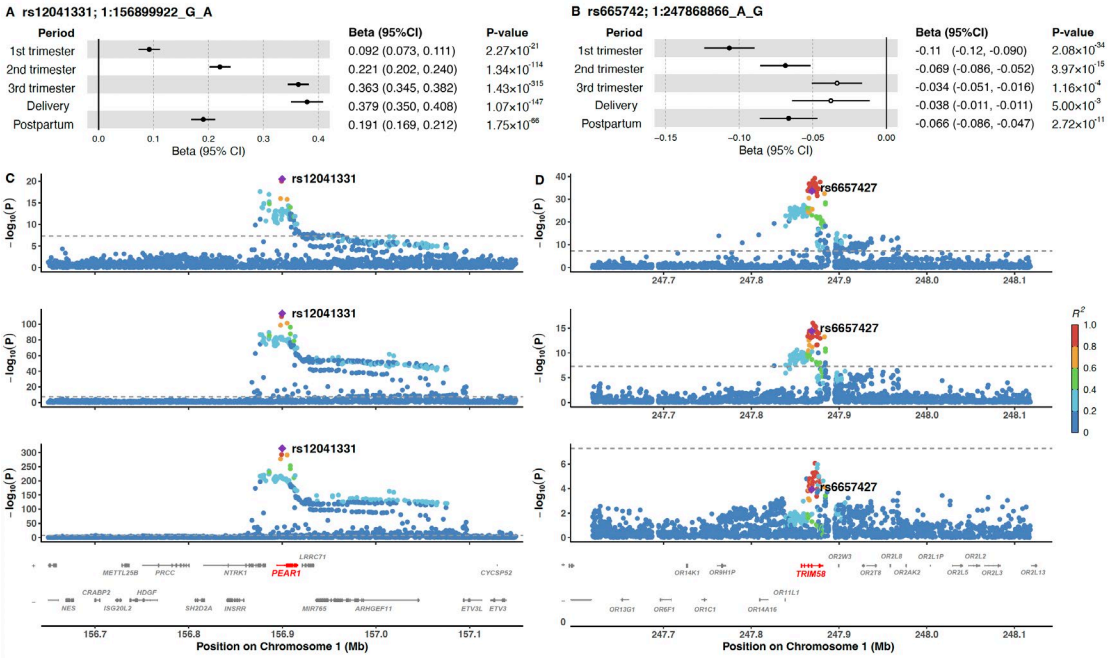

Figure S22. Forest plots and regional association plots for two variants with time-dependent genetic effects for MPV during pregnancy. Forest plots showing the genetic effect of (A) rs12041331-A allele at 1q23.1 (*PEAR1*) and (B) rs6657427-A allele at 1q44 (*TRIM58*) on meta-analysis for platelet count during the first, second, and third trimester, at delivery, and during the postpartum period. Points represent genetic effect (beta). Hollow points indicate a *P* value not reaching genome-wide significance ($P = 5 \times 10^{-8}$). The error bars indicate the 95% confidence interval of beta. Regional association plots from top to bottom represent the results of meta-analyses for platelet count during the first, second, and third trimesters at (C) 1q23.1 (*PEAR1*) and (D) 1q44 (*TRIM58*). The x-axis shows the chromosomal positions (GRCh38) and the y-axis indicates $-\log_{10}$(*P*-value) for the association tests. The purple diamond indicates the lead SNP of each locus. The other SNPs are colored based on their LD r^2 with the lead SNP. The dashed grey line represents the genome-wide significance threshold for GWAS ($P = 5 \times 10^{-8}$). The gene track highlighted in red shows the nearest gene for the lead SNP.

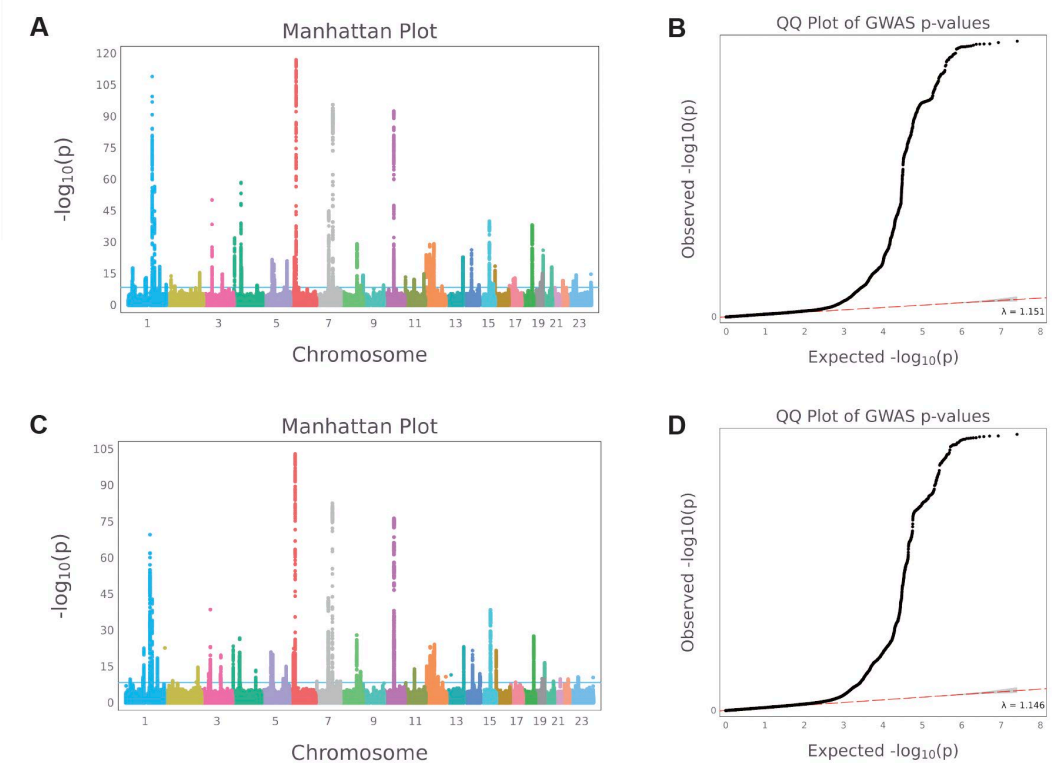

Figure S23. TrajGWAS results of the mean of longitudinal MPV during pregnancy and the postpartum period.

74,013 pregnancies (Longgang: n = 39,546, Baoan: n = 34,467) with more than one MPV during pregnancy and the postpartum period were included in the TrajGWAS analyses. MPVs were rank-based transformed. The first to tenth principal components, age, and gestation age corresponding to the time of the MPV test were adjusted as covariates. Manhattan plots for (A) Longgang and (C) Baoan. The x-axis shows the ordered chromosomes and the y-axis indicates -$\log_{10}$(*P*-value) for the TrajGWAS analyses. The blue horizontal line represents the genome-wide significance threshold ($P = 5\times10^{-8}$). QQ plots for (B) Longgang and (D) Baoan show the observed -$\log_{10}$(*P*-value) in TrajGWAS analyses against expected -$\log_{10}$(*P*-value). The red dashed line indicates the distribution of *P* values under the null hypothesis and the gray shaded area indicates standard errors. MPV: mean platelet volume.

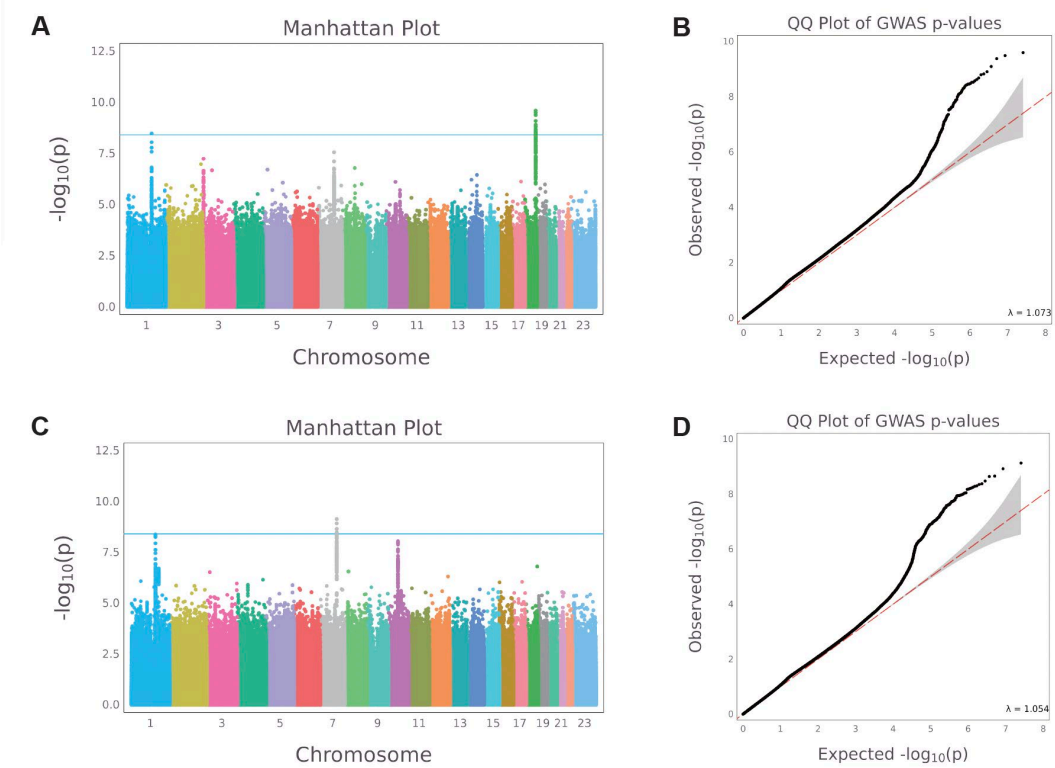

611

612 **Figure S24. TrajGWAS results of the within-subject variability of longitudinal MPV during**

613 **pregnancy and the postpartum period.**

614 74,013 pregnancies (Longgang: n = 39,546, Baoan: n = 34,467) with more than one MPV during

615 pregnancy and the postpartum period were included in the TrajGWAS analyses. MPVs were rank-

616 based transformed. The first to tenth principal components, age, and gestation age corresponding

617 to the time of the MPV test were adjusted as covariates. Manhattan plots for (A) Longgang and

618 (C) Baoan. The x-axis shows the ordered chromosomes and the y-axis indicates -$\log_{10}$(*P*-value)

619 for the TrajGWAS analyses. The blue horizontal line represents the genome-wide significance

620 threshold ($P = 5\times10^{-8}$). QQ plots for (B) Longgang and (D) Baoan show the observed -$\log_{10}$(*P*-

621 value) in TrajGWAS analyses against expected -$\log_{10}$(*P*-value). The red dashed line indicates the

622 distribution of *P* values under the null hypothesis and the gray shaded area indicates standard

623 errors. MPV: mean platelet volume.